



Mission
Performance
Centre



Customer: ESA	Document Ref.: S3MPC.UOL.VR.029
Contract No.: 4000111836/14/I-LG	Date: 30/06/2017
	Issue: 1.0

Project:	PREPARATION AND OPERATIONS OF THE MISSION PERFORMANCE CENTRE (MPC) FOR THE COPERNICUS SENTINEL-3 MISSION
Title:	S3 Validation Report – SLSTR
Author(s):	Darren Ghent, University of Leicester
Distribution:	ESA
Filename	S3MPC.UOL.VR.029 - i1r0 - SLSTR L2 Land Validation Report.docx

Copyright ©2017– ACRI-ST

All rights reserved.

No part of this work may be disclosed to any third party translated, reproduced, copied or disseminated in any form or by any means except as defined in the contract or with the written permission of ACRI-ST

ACRI-ST

260 route du Pin Montard

06904 Sophia-Antipolis, France

Tel: +33 (0)492 96 75 00 Fax: +33 (0)4 92 96 71 17

www.acri-st.fr

Disclaimer

The work performed in the frame of this contract is carried out with funding by the European Union. The views expressed herein can in no way be taken to reflect the official opinion of either the European Union or the European Space Agency.





Changes Log

Version	Date	Changes
1.0	30/06/2017	First version

Table of content

1	INTRODUCTION	1
1.1	SUMMARY.....	1
1.2	REFERENCE DOCUMENTS.....	1
1.2.1	<i>Applicable documents</i>	1
1.2.2	<i>Reference documents</i>	2
1.3	DEFINITIONS.....	4
2	OVERVIEW OF CAL/VAL PLAN	7
2.1	SOURCE OF SLSTR LST DATA	9
2.2	METHODS FOR CATEGORY-A VALIDATION	9
2.3	SATELLITE EXTRACTIONS FOR THE SLMDB	9
2.4	IN SITU OBSERVATIONS FOR THE SLMDB	10
2.5	MATCHUP RATIONALE FOR THE SLMDB	11
2.6	MATCHUPS FROM GLOBTEMPERATURE	11
2.7	METHODS FOR CATEGORY-C VALIDATION	11
2.7.1	<i>Spatiotemporal Matching</i>	12
2.7.2	<i>Evaluation Metrics</i>	13
2.8	DESCRIPTION OF CATEGORY-A REFERENCE DATA.....	13
2.8.1	<i>Gold Standard Stations</i>	13
2.8.2	<i>Complementary Stations</i>	15
2.9	DESCRIPTION OF CATEGORY-C REFERENCE DATA.....	16
2.9.1	<i>GlobTemperature Geostationary Operational Environmental Satellite (GOES) LST Product</i>	16
2.9.2	<i>GlobTemperature MODerate resolution Imaging Spectrometer (MODIS) LST Product</i>	17
2.9.3	<i>GlobTemperature Spinning Enhanced Visible and Infrared Imager (SEVIRI) LST Product</i>	19
3	RESULTS OF CATEGORY-A VALIDATION.....	22
4	RESULTS OF CATEGORY-C VALIDATION	30
4.1	SL_2_LST vs. GLOBTEMPERATURE TERRA-MODIS.....	30
4.2	SL_2_LST vs. GLOBTEMPERATURE GOES (GOES__LST_2).....	35
4.3	SL_2_LST vs. GLOBTEMPERATURE SEVIRI (SEVIR__LST_2)	42
5	CONCLUSIONS AND RECOMMENDATIONS.....	50
5.1	CATEGORY-A VALIDATION.....	50
5.2	CATEGORY-C VALIDATION	50
5.3	RECOMMENDATIONS.....	51
6	ANNEXES	52
6.1	ANNEX I: SLSTR BIOME CLASSES	52
6.2	ANNEX II: USCRN VALIDATION PLOTS	53

List of Figures

Figure 1: Locations of NOAA SURFRAD stations and ARM Southern Great Plains (SGP). Source: NOAA ESRL (<http://www.esrl.noaa.gov/gmd/grad/surfrad/index.html>) -----14

Figure 2: Locations of the USCRN stations over the contiguous United States (<https://www.ncdc.noaa.gov/crn/map.html>) -----15

Figure 3: Validation of the SL_2_LST product over the mid-July to mid-November reprocessed period at three Gold Standard in situ stations managed by the Karlsruhe Institute of Technology: Evora, Portugal (left); Gobabeb, Namibia [centre]; Kalahari-Heimat, Namibia (right). [Results courtesy of Maria Martin through the GlobTemperature Project]-----22

Figure 4: Validation of the SL_2_LST product over the mid-July to mid-November reprocessed period at the seven Gold Standard in situ stations of the SURFRAD network plus a Gold Standard station from the ARM network: Bondville, Illinois top-(left); Desert Rock, Nevada [top-centre]; Fort Peck, Montana (top-right); Goodwin Creek, Mississippi (middle-left); Penn State University, Pennsylvania (middle-centre); Sioux Fall, South Dakota (middle-right); Table Mountain, Colorado (bottom-left); and Southern Great Plains, Oklahoma (bottom-centre). -----24

Figure 5: Monthly median Global SNO LST differences between SL_2_LST and GlobTemperature Terra-MODIS for August 2016 (left), September (centre) and October (right). Daytime differences are in the top row and night-time differences in the bottom row. -----31

Figure 6: Monthly median (bars) and robust standard deviation (points) Global SNO LST differences between SL_2_LST and GlobTemperature Terra-MODIS with respect to elevation classes for August 2016 (left), September (centre) and October (right). Daytime differences are in the top row and night-time differences in the bottom row.-----33

Figure 7: Monthly median (bars) and robust standard deviation (points) Global SNO LST differences between SL_2_LST and GlobTemperature Terra-MODIS with respect to SLSTR land cover classes for August 2016 (left), September (centre) and October (right). Daytime differences are in the top row and night-time differences in the bottom row. -----34

Figure 8: Monthly median Global SNO LST differences between SL_2_LST and GlobTemperature Terra-MODIS with respect to SLSTR viewing geometry for August 2016 (left), September (centre) and October (right). Daytime differences are in red and night-time differences in blue.-----35

Figure 9: Monthly median SNO LST differences for North America between SL_2_LST and GlobTemperature GOES for August 2016 (left), September (centre) and October (right). Daytime differences are in the top row and night-time differences in the bottom row. -----37

Figure 10: Monthly median (bars) and robust standard deviation (points) SNO LST differences for North America between SL_2_LST and GlobTemperature GOES with respect to elevation classes for August 2016 (left), September (centre) and October (right). Daytime differences are in the top row and night-time differences in the bottom row.-----39

Figure 11: Monthly median LST uncertainties for North America from GlobTemperature GOES for August 2016 (left), September (right). Daytime uncertainties are in the top row and night-time uncertainties in the bottom row. -----40

Figure 12: Monthly median (bars) and robust standard deviation (points) SNO LST differences for North America between SL_2_LST and GlobTemperature GOES with respect to SLSTR land cover classes for August 2016 (left), September (centre) and October (right). Daytime differences are in the top row and night-time differences in the bottom row. -----41

Figure 13: Monthly median SNO LST differences for North America between SL_2_LST and GlobTemperature GOES with respect to SLSTR viewing geometry for August 2016 (left), September (centre) and October (right). Daytime differences are in red and night-time differences in blue. -----42

Figure 14: Monthly median SNO LST differences for Europe between SL_2_LST and GlobTemperature SEVIRI for August 2016 (left), September (centre) and October (right). Daytime differences are in the top row and night-time differences in the bottom row. -----44

Figure 15: Monthly median (bars) and robust standard deviation (points) SNO LST differences for Europe between SL_2_LST and GlobTemperature SEVIRI with respect to elevation classes for August 2016 (left), September (centre) and October (right). Daytime differences are in the top row and night-time differences in the bottom row. -----46

Figure 16: Monthly median LST uncertainties for Europe from GlobTemperature SEVIRI for August 2016 (left), September (right). Daytime uncertainties are in the top row and night-time uncertainties in the bottom row. -----47

Figure 17: Monthly median (bars) and robust standard deviation (points) SNO LST differences for Europe between SL_2_LST and GlobTemperature SEVIRI with respect to SLSTR land cover classes for August 2016 (left), September (centre) and October (right). Daytime differences are in the top row and night-time differences in the bottom row. -----48

Figure 18: Monthly median SNO LST differences for Europe between SL_2_LST and GlobTemperature SEVIRI with respect to SLSTR viewing geometry for August 2016 (left), September (centre) and October (right). Daytime differences are in red and night-time differences in blue. -----49



List of Tables

Table 1: Gold Standard stations used in the primary validation of the SL_2_LST product. [*Note: The KIT managed stations (shaded in grey) are included here through GlobTemperature Validation as part of the collaboration between S3MPC and ESA DUE GlobTemperature; actual matchups are provided courtesy of Maria Martin] -----	14
Table 2: Overview information for the GlobTemperature GOES LST products reproduced from [RD-11]	16
Table 3: Overview information for the GlobTemperature Terra-MODIS “value-added” LST products made available via the GlobTemperature Data Portal reproduced from [RD-11] -----	18
Table 4: Overview information for the GlobTemperature SEVIRI LST products made available via the GlobTemperature Data Portal reproduced from [RD-11]-----	20
Table 5: Validation of the SL_2_LST product over the mid-July to mid-November reprocessed period at the three Gold Standard in situ stations managed by the Karlsruhe Institute of Technology, and the eight Gold Standard sites of the SURFRAD and ARM networks.-----	26
Table 6: Validation of the SL_2_LST product over the mid-July to mid-November reprocessed period at select USCRN in situ stations.-----	27

1 Introduction

1.1 Summary

This is a Validation Report for the release of Sentinel-3 Sea and Land Surface Temperature Radiometer (SLSTR) Level-2 Land Surface Temperature product (SL_2_LST). The Report describes the validation of SL_2_LST against in situ observations (Category-A validation), and intercomparison (Category-C validation) of the SL_2_LST product with respect to three independent reference products from the ESA DUE GlobTemperature Project (MODIS, GOES, and SEVIRI).

The results of the validation (Category-A) against in situ observations from “Gold Standard” stations show the SL_2_LST product to have an accuracy for all matchups of 0.94 K, thus meeting the overall mission requirement (S3-MR-420) of < 1 K. Intercomparison (Category-C) with respect to other reference products show differences are around 1 K overall.

1.2 Reference documents

1.2.1 Applicable documents

Id	Title
AD-1	SLSTR L2 Land Surface Temperature Product Notice, ref. S3A.PN-SLSTR-L2L.02, dated on 30/06/2017
AD-2	Sentinel-3 CAL/VAL Plan, ref. 3MPC.ACR.PLN.008
AD-3	SLSTR L2 Land Surface Temperature ATBD, ref. S3-L2-SD-03-T03-ULNILU-ATBD-L2LST, dated on 10/10/2012
AD-4	University of Leicester Thermal Infrared Probabilistic Cloud Detection for Land ATBD, ref. S3-ATBD_UOL_CLOUDS_V3, dated on 20/09/2016

1.2.2 Reference documents

Id	Title
RD-1	Schneider, P., Ghent, D., Corlett, G., Prata, F., and Remedios, J. <i>Land Surface Temperature Validation Protocol (Report to European Space Agency)</i> . 2012 (UL-NILU-ESA-LST-LVP).
RD-2	Jallego, F. J., Stratified sampling of satellite images with a systematic grid of points. <i>ISPRS Journal of Photogrammetry and Remote Sensing</i> , 2005. 59(6): p. 369-376.
RD-3	Ghent et al., <i>GlobTemperature Technical Specification i2r1 (Report to European Space Agency)</i> . 2016
RD-4	Ghent et al., <i>GlobTemperature Technical Note on Common Nomenclature i1r0 (Report to European Space Agency)</i> . 2016
RD-5	Joint Committee for Guides in Metrology, <i>Evaluation of Measurement Data - Guide to the Expression of Uncertainty in Measurement</i> . 2008.
RD-6	CEOS, <i>Committee on Earth Observation Satellites</i> (http://www.ceos.org/).
RD-7	Ghent, D., <i>Land Surface Temperature Validation and Algorithm Verification (Report to European Space Agency)</i> . 2012 (UL-NILU-ESA-LST-VAV).
RD-8	Martin, M., Gottsche F, Ghent D, Trent, T., Dodd, E., Pires A, Trigo I, Prigent C, Jimenez, C, and Remedios. J., <i>ESA DUE GlobTemperature Satellite LST Intercomparison Report i2r1 (Report to European Space Agency)</i> 2016
RD-9	Trigo, I.F., et al., <i>An assessment of remotely sensed land surface temperature</i> . <i>J. Geophys. Res.</i> , 2008a. 113 (D17108).
RD-10	GCOS 2016 Implementation Plan (GCOS-200)
RD-11	Ghent et al., <i>GlobTemperature Product User Guide (PUG) i2r1 (Report to European Space Agency)</i> . 2016
RD-12	Yu, Y., et al, <i>Developing algorithm for operational GOES-R land surface temperature product</i> , <i>IEEE Trans. Geosci. Remote Sens.</i> , vol. 47, no. 3, pp. 936-951, 2009
RD-13	Wan, Z., <i>New refinements and validation of the MODIS land surface temperature/emissivity products</i> . <i>Remote Sensing of Environment</i> , 2008. 112: p. 59–74.
RD-14	Wan, Z. and J. Dozier, <i>A generalized split-window algorithm for retrieving land surface temperature from space</i> . <i>IEEE Transactions on Geoscience and Remote Sensing</i> , 1996. 34: p. 892–905.
RD-15	Seemann, S.W., et al., <i>Development of a global infrared land surface emissivity database for application to clear sky sounding retrievals from multispectral satellite radiance measurements</i> . <i>Journal of Applied Meteorology and Climatology</i> , 2008. 47(1): p. 108-123.

Id	Title
RD-16	Trigo, I.F., et al., The Satellite Application Facility on Land Surface Analysis. <i>Int. J. Remote Sens.</i> , 2011. 32: p. 2725-2744.
RD-17	Freitas, S.C., et al., Quantifying the Uncertainty of Land Surface Temperature Retrievals From SEVIRI/Meteosat. <i>IEEE Trans. Geosci. Remote Sens.</i> , 2010.
RD-18	Trigo, I.F., et al., An assessment of remotely sensed land surface temperature. <i>J. Geophys. Res.</i> , 2008a. 113(D17108).
RD-19	Augustine, J.A., J.J. DeLuisi, and C.N. Long, SURFRAD—A National Surface Radiation Budget Network for Atmospheric Research. <i>Bulletin of the American Meteorological Society</i> , 2000. 81(10): p. 2341-2357.
RD-20	Yunyue, Y., et al., <i>Validation of GOES-R Satellite Land Surface Temperature Algorithm Using SURFRAD Ground Measurements and Statistical Estimates of Error Properties</i> . <i>Geoscience and Remote Sensing, IEEE Transactions on</i> , 2012. 50(3): p. 704-713.
RD-21	Wang, K. and S. Liang, <i>Evaluation of ASTER and MODIS land surface temperature and emissivity products using long-term surface longwave radiation observations at SURFRAD sites</i> . <i>Remote Sensing of Environment</i> , 2009. 113(7): p. 1556-1565.
RD-22	Cuenca, J. and J.A. Sobrino, <i>Experimental Measurements for Studying Angular and Spectral Variation of Thermal Infrared Emissivity</i> . <i>Applied Optics</i> , 2004. 43(23): p. 4598-4602.
RD-23	Sobrino, J.A. and J. Cuenca, <i>Angular Variation of Thermal Infrared Emissivity for Some Natural Surfaces from Experimental Measurements</i> . <i>Applied Optics</i> , 1999. 38: p. 3931–36.
RD-24	Martin, M., Gottsche F, Ghent D, and Remedios. J., <i>ESA DUE GlobTemperature Satellite LST Validation Report i2r1 (Report to European Space Agency) 2016</i>
RD-25	Götttsche, F.-M., F.-S. Olesen, and A. Bork-Unkelbach, <i>Validation of land surface temperature derived from MSG/SEVIRI with in situ measurements at Gobabeb, Namibia</i> . <i>Int. Journal of Remote Sensing</i> , 2013. 34 (9-10): p. 3069-3083.
RD-26	Götttsche, F.-M., F.S. Olesen, I.F. Trigo, A. Bork-Unkelbach, and M.A. Martin, <i>Long Term Validation of Land Surface Temperature Retrieved from MSG/SEVIRI with Continuous in-Situ Measurements in Africa</i> . <i>Remote Sensing</i> , 2016. 8(5), n° 410: p. 1 -27.
RD-27	Noyes, E.J. (2006). <i>Technical Assistance for the Validation of AATSR Land Surface Temperature Products, Final Report - February 2006 (Report to European Space Agency)</i>
RD-28	NOAA/NESDIS, 2007. <i>United States Climate Reference Network (USCRN) Functional Requirements Document (No. NOAA-CRN/OSD-2003-0009R1UD0)</i> . U.S. Department of Commerce, National Oceanic and Atmospheric Administration (NOAA), National Environmental Satellite, Data, and Information Service (NESDIS).
RD-29	USCRN Network, https://www.ncdc.noaa.gov/data-access/land-based-station-data/land-based-datasets/us-climate-reference-network-uscrn
RD-30	Götttsche, F.-M., and G.C. Hulley, <i>Validation of six satellite-retrieved land surface emissivity products over two land cover types in a hyper-arid region</i> . <i>Remote Sensing of Environment</i> , 2012. 124: p. 149-158.

Id	Title
RD-31	Jimenez-Munoz, J.C., et al., Temperature and Emissivity Separation From MSG/SEVIRI Data. Geoscience and Remote Sensing, IEEE Transactions on, 2014. 52(9): p. 5937-5951.
RD-32	Cheng, J., S. Liang, Y. Yao, and X. Zhang, Estimating the optimal broadband emissivity spectral range for calculating surface longwave net radiation. IEEE Geoscience and Remote Sensing Letters, 2013. 10: p. 401–405.

1.3 Definitions

In order for a consolidated understanding of the validation metrics presented in this report it is pertinent to adhere to a consistent set of definitions related to validation of LST products. These definitions are taken from the GlobTemperature Technical Note on Common Nomenclature [RD-4], which itself adopts as a baseline definitions from the growing source of literature on LST, and in particular from [RD-5], which is the standard for Metrology nomenclature. In order to achieve community acceptance of the nomenclature presented here, the definitions were iterated with the International LST & Emissivity Working Group (ILSTE); this being a representative sample of the view of the wider data provider, LST expert, and user communities.

Terminology	Definition	Comments
Absolute bias	A systematic error between a measurement and the true value [RD-5]	This is of theoretical importance only here, as the exact true value of LST cannot be known due to measurement error
Accuracy	Accuracy can be thought of as the degree of conformity of the measurement of a quantity to the accepted value or the “true” value [RD-5]	
Calibration	Calibration is the process of quantitatively defining the system response to known, controlled system inputs [RD-1]	It may involve the subsequent implementation of correction factors from ground or in-flight calibration to transform the measured signals in a satellite instrument to calibrated radiances
Discrepancy	Discrepancy describes the lack of similarity between two measurements, where this is outside some expected error bound. [RD-1]	

Terminology	Definition	Comments
Error	Result of a measurement minus a true value of the measurand [RD-5]	Note that in practice, at least for LST, a true value cannot be determined and therefore a conventional true value is used instead
Ground Truth	In situ measurements of a measurand	However, this term is generally not used because in situ measurements are not actually 'truth'
Intercomparison	The process of comparing two or more (LST) data sets to allow evaluation of their relative consistency [RD-1]	
Measurand	A measurand is the particular quantity subject to measurement [RD-5]	
Precision	Precision is the closeness of agreement between independent measurements of a quantity under the same conditions [RD-5]	
Random error	Result of a measurement minus the mean that would result from an infinite number of measurements of the same measurand carried out under repeatability conditions [RD-5]	
Reference standard	Measurement standard designated for the calibration "in situ" of other (similar) measurement systems. Usually applied to instruments of a given kind or at a given location for which the reference standard has been agreed to be relevant [RD-1]	
Relative bias	A systematic error between measurements obtained from different data sources [RD-1]	
Relative error	The relative error is the error of measurement divided by a true value of the measurand [RD-1]	
Systematic error	Mean that would result from an infinite number of measurements of the same measurand carried out under repeatability conditions minus a true value of the measurand [RD-1]	

Terminology	Definition	Comments
True value	A true value is the value consistent with the definition of a given particular quantity [RD-1]	
Uncertainty	A parameter associated with the result of a measurement, that characterizes the dispersion of the values that could reasonably be attributed to the measurand, that is the value of the particular quantity to be measured [RD-5]	
Validation	The process of assessing, by independent means, the quality of a given set of data products [RD-6]	Primarily this is an assessment of the accuracy using equivalent in situ observations, but can refer to intercomparison and radiance-based assessment
Validation loop	The validation loop describes the iterative process between algorithm development and validation, where validation findings are investigated and reflected in algorithm changes with the final goal of improving the output product [RD-1]	

2 Overview of CAL/VAL Plan

The CAL/VAL Plan for the MPC Commissioning Phase – OPT [AD-2] describes the activities to be carried out to ensure the Sentinel-3A SLSTR Level-2 Land Surface Temperature product (SL_2_LST) is fit to be deployed in the land processing centres for operational release to the user community.

2.1 Objectives

Covered requirements: [SLSTR-LST-CV-200]

The objective of this requirement is to coordinate all LST validation activities, both within the MPC and externally within the S3VT-L team; the overall aim of which is to demonstrate that the SLSTR-LST product complies with mission requirements S3-MR-420 and S3-MR-430.

- ❖ S3-MR-420: Sentinel-3 shall be able to measure Land Surface Temperature (LST) to an accuracy of < 1K with a resolution of 1 km at nadir. This capability shall not reduce the quality of the SST retrievals.
- ❖ S3-MR-430: Sentinel-3 shall be able to measure Ice Surface Temperature (IST) to an accuracy of 10% with a resolution of < 5 km (1 km goal) at nadir. This capability shall not reduce the quality of the SST retrievals.

Covered requirements: [SLSTR-LST-CV-210]

The objective of this requirement is to set-up the tools and methods for the validation of the SLSTR LST products. This is to include the generation of both in situ vs. SLSTR matchups, simulated LST from radiative transfer vs. SLSTR matchups, and SLSTR vs. other satellite matchups from a matchup engine. These matchups will form the SLSTR LST Matchup Database (SLMDB). The MDB will store all available L1b and L2 fields from SLSTR, and either all equivalent input data from other satellite sensors for intercomparisons, all simulated data including meteorological variables for radiance-based validation, or all available and necessary in situ data from site measurements.

2.2 Validation Approach

The four-phase approach of the LST Validation Protocol [RD-1], which has become the established set of guidelines for rigorous LST validation is followed. This has been adopted by existing projects for their validation activities, such as for ESA DUE GlobTemperature; and is the baseline for the CEOS-LPV “Best Practices” guidelines.

The approach specifies the following four categories of validation:

- ❖ **Category-A:** Comparison of satellite-retrieved LST with in situ measurements collected from radiometers sited at a number of stations spread across the Earth, for which the highest-quality validation can be achieved.
- ❖ **Category-B:** Radiometric-based validation, which offers an alternative to validation with in situ LST measurements as it does not require measurements of LST on the ground, and can provide a viable alternative for long-term, semi-operational LST product evaluation at the global scale;
- ❖ **Category-C:** Inter-comparisons with similar LST products from other sources such as AATSR, AVHRR, MODIS, SEVIRI, and VIIRS, which give important quality information with respect to spatial patterns in LST deviations;
- ❖ **Category-D:** Time series analysis to quantify trends and to identify potential instrument drift or persistent cloud contamination.

2.3 Status of SLSTR LST Matchup Database (SLMDB)

The core of the SLMDB are the pre-existing scientific tools from the University of Leicester (UoL) LST validation toolbox. This supports the storage and processing of extracted satellite data with respect both to in situ observations and with each other. An identified gap here has been the routine extractions of the SL_2_LST product. The objective remains for this to be provided via a CFI such as MERMAID or Felyx. In this case the decision has been taken to utilize adapted functionality in MERMAID, though this has yet to go operational in the validation loop.

For the purposes of this report the SL_2_LST extractions have been made through new code embedded in the UoL LST validation toolbox. While we wait for visualisation tools for analysis of matchups, which are required for routine generation of reports and other presentation material, this capability has been provided by adapted scientific code from the UoL LST validation toolbox.

The format of the current extractions conform to two different types:

- ❖ Level-2 subsets of 51 x 51 pixels centred on the in situ station
- ❖ Level-3 uncollated (L3U) PDUs, which are averaged LST data from the input Level-2 PDUs; the averaging being in space but not time

With no Level-3 averaging tool yet available, equivalent software in the UoL LST validation toolbox has been adapted for use in the SLMDB. Hence, in this version of the SLSTR LST Validation Report we focus on Categories-A and –C for which we have the adapted software. Adaptions to the software for Category-B validation is currently in development and will be incorporated into the next version of the Report; and Category-D validation will be carried out once we have a sufficiently long data record which covers the full intra-annual cycle.

2.4 Source of SLSTR LST Data

For this report we use SLSTR data provided through the S3-MPC and made available to the S3VT community. Specifically, these data are reprocessed Level-1 and Level-2 PDUs (granules) starting on 12th July 2016 through to 15th November 2016. For this reprocessing the processing baseline was PB2.10.

This selection is justified since it provides both full months of SL_2_LST data, and the processing baseline used (PB2.10) is consistent with the latest pre-operational release processing baseline (PB2.16) in terms of LST algorithm implementation (IPF and ADFs).

The basic cloud mask has seen modifications between these processing baselines, but data from PB2.10 through to PB2.16 is not consistent in terms of LST processing implementation. Specifically PB2.14 saw a backward implementation of a set of pre-launch ADFs thus making the data unusable. The processing chain has subsequently been corrected and PB2.16 now has the correct implementation as per PB2.10. Since the PB2.10 cloud masking shows more over-flagging than PB2.16 the effect on the validation statistics is expected to be minimal.

2.5 Methods for Category-A Validation

For the Category-A validation we define 2 sub-classes of ground-based sites:

- ❖ “Gold Standard” stations which are well characterised and calibrated, and for which the location of the sites are specially selected for LST validation. These include: the sites managed by the Karlsruhe Institute of Technology (KIT); and SURFRAD stations and a select Atmospheric Radiation Measurement (ARM) station, which use well calibrated instrumentation and provide long-time series of in situ observations.
- ❖ Complementary stations, which while being well calibrated are equipped with lower quality thermal infrared instrumentation. These were not designed for LST validation, but robust selection of the most appropriate sites can increase our validation statistics.

2.5.1 Satellite extractions for the SLMDB

Prior to the matchup process all LST extractions for each validation site are generated. Briefly, this process involves:

- ❖ For each SLSTR granule, determining whether the orbit overpasses the validation station
- ❖ Where a SLSTR granule overpasses a station an extract of 51 x 51 pixels is made centred on the position of the in situ station
- ❖ Storing all required data together with auxiliary fields relevant to the LST retrieval for evaluation of the validation results with respect to metrics

- ❖ All extracted satellite pixels are cloud cleared using the most appropriate of the SLSTR basic cloud masks, which in this case is the summary cloud mask

2.5.2 In situ observations for the SLMDB

The ground-based observations using radiometers or pygeometers are all positioned within a few metres of the surface and thus atmospheric attenuation of the surface-leaving radiance can be neglected. For in situ measurements taken at the surface of the earth with IR radiometers, the surface temperature (T_{sfc}) can be solved using the equation:

$$B_c(T_c) = \epsilon_c B_c(T_{sfc}) + ((1 - \epsilon_c) B_c(T_{sky}))$$

Where $B_c(T_c)$ is the emitted radiance given by the Planck function for an effective brightness temperature in the radiometer channel c , $B_c(T_{sfc})$ is the emitted radiance given by the Planck function for a surface temperature T_{sfc} , ϵ_c is the emissivity of the Earth's surface in the radiometer channel c , and $B_c(T_{sky})$ is the down-welling atmospheric radiance given by the Planck function for an effective brightness temperature of the atmosphere. The downwelling radiance is measured by an additional sky-facing radiometer. For narrow-band radiometers the equivalent channel-effective emissivities are used from in situ measurements [RD-30] or from satellite datasets such as MSG/SEVIRI [RD-31].

For SURFRAD sites which measure broadband upwelling and downwelling radiation we need associated broadband emissivities (BBEs) in order to determine the in situ LST. We do this in a two-step procedure. First, emissivities at distinct values ("hinge points") are acquired at a spatial resolution of 0.05° from the CIMMS Baseline Fit Emissivity Database [RD-15]. Second, the BBE is then calculated in the spectral range of $8 - 13.5 \mu\text{m}$ following the formula of [RD-32]:

$$\text{BBE} = 0.068 + 0.045\epsilon_6 + 0.297\epsilon_7 + 0.215\epsilon_8 + 0.372\epsilon_9$$

where ϵ_6 , ϵ_7 , ϵ_8 and ϵ_9 are the emissivities at the respective hinge points: 8.3, 9.3, 10.8 and $12.1 \mu\text{m}$. Since CIMMS emissivity data are not available in near real time we use mean monthly estimates from climatology.

2.5.3 Matchup rationale for the SLMDB

The methodology of matching the in situ observations with the satellite extractions can be summarised as follows:

- ❖ Each site individually evaluated for representativeness. The spatial matching is performed on a site specific basis. The station is located in the centre pixel of the 51×51 satellite extraction. Where this central pixel is representative of the Field of View (FOV) of the in situ radiometer then this single pixel is selected for the matchup. For very heterogeneous surfaces it is

assessed whether an alternative pixel(s) selection is more representative. This can be for 3 x 3 or 5 x 5 pixels centred on the in situ station, or selected pixel(s) offset from the station location but being more representative. Where several pixels are selected, the median LST of the cloud cleared pixels is used.

- ❖ Where in situ observations are not exactly matched temporally with the scan time(s) of SLSLSTR for the selected pixel(s) then linear interpolation between the two station measurements that are closest to the scan time(s) is performed. For SURFRAD for example the temporal difference between SLSTR matched pixel(s) and in situ acquisition is less than 30 seconds.
- ❖ In the analyses separate metrics are determined for day and night matchups, where day / night is determined by the solar zenith angle.
- ❖ Examination of individual matchups find that cloud contamination remains problematic, and to minimise this impact we apply an additional cloud filtering. This is set as a 3σ threshold.

2.5.4 Matchups from GlobTemperature

To supplement the routine matchups being produced within the SLMDB we include here validation in the framework of ESA DUE GlobTemperature with respect to high-quality in situ observations made available by the Karlsruhe Institute of Technology (KIT). The SLSTR extractions are made in the same way from within the SLMDB software. The preparation of the in situ data and the satellite vs. in situ matchups are performed by KIT within GlobTemperature. The methodology for these matchups is in general consistent with the approach used in the SLMDB – both of which follow the procedures of [RD-1]. A full description of the per site matching is provided in [RD-24].

2.6 Methods for Category-C Validation

For comprehensive intercomparison covering all possible surface types and a broader range of atmospheres products are compared over both continental regions (North America and Europe) and over the full globe. The first supports both Low Earth Orbit (LEO) vs. LEO and LEO vs. Geostationary Earth Orbit (GEO) comparisons, whereas the second enables comparison of simultaneous nadir overpasses of LEO vs. LEO.

2.6.1 Spatiotemporal Matching

For a useful intercomparison of data sets from different satellites, the spatial variability within the field of view of each satellite needs to be accounted for. This can be achieved by re-gridding the data onto a common spatial grid by averaging all geo-referenced, cloud free pixels weighted by their respective fractional area overlap with the corresponding common grid cell. For matchups between data sets with

different spatial resolutions or different orbital tracks, the standard spatial resolution for re-gridding is defined as $0.05^\circ \times 0.05^\circ$ for comparisons between Thermal Infrared (TIR) LST products.

There are several methods for the spatial matching of two satellite data sets. The so-called nearest neighbour approach is an effective and relatively straightforward method. The images of the two considered satellites are overlaid with each other by shifting one set of pixels so that they match the other set. The advantage of the method is that no data is averaged or weighted, thus the original data remains unchanged and the two original data sets are compared. However, the larger the shift gets, the further apart the compared LST values are spatially. A second approach is the averaging of the data by polygon weighting. A polygon tessellation is formed and to account for the fact that the pixel area and the area of interest are often not exactly the same, the data in each polygon is weighted according to the proportion of the area of interest in the polygon to its total area (see e.g [RD-2]).

The optimal approach taken here is to apply the polygon weighting. The rationale being that a high spatial resolution matchup grid would be highly sensitive to LEO orbit tracks and their pixel nearest neighbour binning. This is particularly the case at the edge-of-swath of wide-swath instruments such as MODIS where pixel sizes are similar in size to the common matchup grid. All matchups adhere to this common approach.

The high temporal variability of LST ensures that intercomparison of different LST products is a challenging prospect. In order to minimise the impact on the intercomparison results, LST differences due to deviating observation times have to be minimised. This can be achieved by limiting the data to close temporal matchups. To maintain consistency no interpolation between adjacent GEO LSTs that temporally bracket a specific LEO overpass time, as has been applied in some studies, is carried out here. Moreover, interpolation between less frequent GEO observations increases the risk that any assumption of a linear relationship between bracketing LST observations becomes invalid. The defined temporal matchup threshold is set to 7.5 minutes consistent with the approach in GlobTemperature [RD-3]. Larger thresholds increase the risk of LST differences representing actual ground temperature changes rather than that they are attributable to the products themselves, while smaller thresholds reduce the number of actual matchups thereby impacting the statistical significance of the results.

Prior to the matchup procedure all input data is processed into Level-3 uncollated (L3U) datafiles on the common matchup grid. These are orbit / granule level data gridded in space but not time and therefore preserves the acquisition times. These datafiles represent the baseline for all matchups and for higher-level (Level-3 collated (L3C) products. All matchups within the 7.5 minute temporal threshold are therefore generated at the L3U product level, and then temporally collated into daytime and night-time composites, where observations are categorised as “day” or “night” based on their respective solar zenith angles.

2.6.2 Evaluation Metrics

A few primary metrics are used in the analysis to better interpret the differences between products. In previous studies [RD-7; RD-8; RD-9] the key metrics have been:

- ❖ satellite viewing geometry
- ❖ orography
- ❖ surface type

We use these same three metrics here, with surface type classified in a consistent manner using the SLSTR biome classification. These provide evidence on how respective algorithms differ in their treatment of the atmosphere, and surface characteristics such as emissivity and elevation.

The data are evaluated with respect to the difference and standard deviation (STD). Difference is defined as the median of the LST product of interest (in this case SL_2_LST) minus a reference LST product. Data are composited over each month where composites are the averages of the individual matchup data.

In the assessment by satellite viewing geometry, differences are binned and analysed against the product of the satellite zenith angle (satze) and the sign of the satellite azimuth angle (sataz) ($\text{satze} * (|\text{sataz}|) / \text{sataz}$).

2.7 Description of Category-A Reference Data

2.7.1 Gold Standard Stations

A principle source of routine “Gold Standard” in situ observations are the SURFRAD (Surface Radiation) network. This was established in 1993 through the support of NOAA's Office of Global Programs and has been operational since 1995 [RD-19; RD-20]. Its primary objective is to support climate research with accurate, continuous, long-term measurements pertaining to the surface radiation budget over the United States [RD-21]. The U.S. Department of Energy's Atmospheric Radiation Measurement (ARM) site Southern Great Plains (SGP_C1) central facility, Lamont, Oklahoma (<http://www.arm.gov/sites/sgp/C>), is also identified as appropriate for LST validation. The station is equipped with Infrared Thermometers (IRT) Wintronics (Heitronics KT15) and it is located in a large area with cattle pasture and wheat fields (Figure 1).



Figure 1: Locations of NOAA SURFRAD stations and ARM Southern Great Plains (SGP). Source: NOAA ESRL (<http://www.esrl.noaa.gov/gmd/grad/surfrad/index.html>)

A key source for ground-based validation data through the link with ESA DUE GlobTemperature has been the well-established LST validation sites managed by the Karlsruhe Institute of Technology (KIT) in Evora (Portugal), Gobabeb (Namibia, Namib desert) and Heimat Farm (Namibia, Kalahari).

The core instruments at these stations are Heitronics KT-15.85 IIP infrared radiometers. Relevant end-members are observed under a view angle of 30°; using this view angle instead of the nadir view is justified by the fact that the angular emissivity variation of sand, grass, and gravel is negligible up to view angles of at least 30° [RD-22; RD-23]. From 25m height the KT-15's full view angle of 8.5° results in a FOV of about 14 m². An additional KT-15 faces the sky at 53° with respect to zenith and measures the channel-specific downwelling longwave radiance, which is used to correct for the reflected component in the down-looking measurements. Full descriptions are available in [RD-3; RD-24; RD-25; RD-26].

Table 1: Gold Standard stations used in the primary validation of the SL_2_LST product. [*Note: The KIT managed stations (shaded in grey) are included here through GlobTemperature Validation as part of the collaboration between S3MPC and ESA DUE GlobTemperature; actual matchups are provided courtesy of Maria Martin]

Code	Name	Latitude	Longitude	Elevation
BON___	Bondville, Illinois	40.05155	-88.37325	230 m
TBL___	Table Mountain, Boulder, Colorado	40.12557	-105.23775	1689 m
DRA___	Desert Rock, Nevada	36.62320	-116.01962	1007 m
FPK___	Fort Peck, Montana	48.30798	-105.10177	634 m
GWN___	Goodwin Creek, Mississippi	34.2547	-89.8729	98 m
PSU___	Penn. State Univ., Pennsylvania	40.72033	-77.93100	376 m
SXF___	Sioux Falls, South Dakota	43.73431	-96.62334	473 m
SGP_C1	Southern Great Plains Facility, Oklahoma	36.605° N	97.485° W	318 m
EVO___	Evora, Portugal	38.540244	-8.003368	230 m
GBB_W_	Gobabeb wind tower, Namibia	-23.550956	15.05138	406 m
KAL_H	Farm Heimat, Kalahari, Namibia	-22.932827	17.992137	1380 m

2.7.2 Complementary Stations

The U.S. Climate Reference Network (USCRN) [RD-28] provides continuous surface temperature data at over 100 stations located within the continental United States and is planned to be operated for many decades in order to provide consistent datasets for climate research. These stations are managed, and maintained by NOAA; and in addition to surface radiometric temperature observations, they also provide measurements of meteorological variables such as surface air temperature, relative humidity, precipitation, and solar radiation.

Station locations are selected to be in environments expected to be free of development for many decades, and are monitored and maintained to high standards with annual calibration carried out [RD-29].

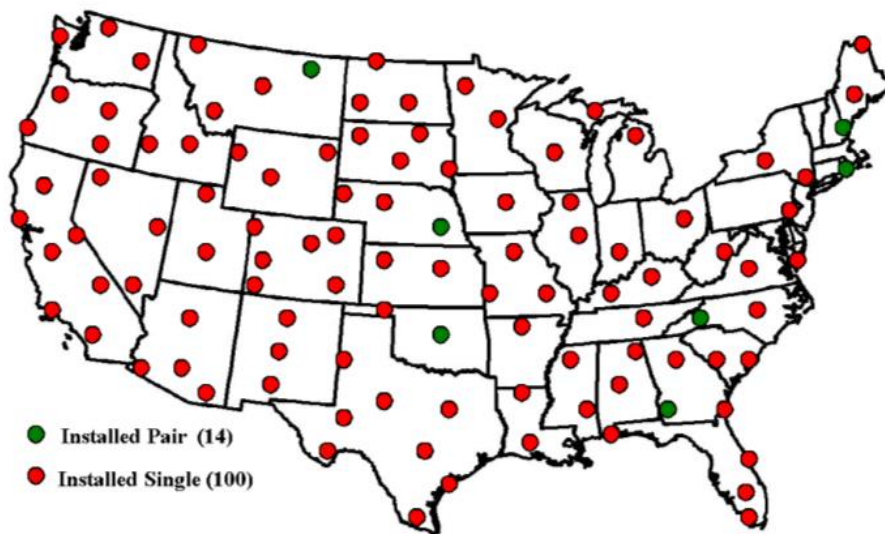


Figure 2: Locations of the USCRN stations over the contiguous United States
(<https://www.ncdc.noaa.gov/crn/map.html>)

The instruments deployed at these stations to measure surface temperature are Apogee Instruments SI-111 infrared radiometers. These measure the surface leaving radiance between 8 and 14 μm . These sensors are calibrated by the manufacturers to a custom black-body cone. Their resultant uncertainty is ± 0.2 C from -15°C to 35°C when the sensor temperature is within 20 K of the surface being measured. The sensor is sampled every second and averaged every 5-minutes. At each station the instrument is placed pointing vertically downwards typically on a 3 meter instrument tower at 1.5 meters above the surface.

2.8 Description of Category-C Reference Data

2.8.1 GlobTemperature Geostationary Operational Environmental Satellite (GOES) LST Product

The GlobTemperature Geostationary Operational Environmental Satellite (GOES) LST Product (GOES__LST_2) is the same product that is produced within the Copernicus Global Land Service. The subsequent description of this product is taken from the GlobTemperature Product User Guide [RD-11].

The Copernicus Global Land Service generates GOES hourly LST data, which are combined with MTSAT and SEVIRI hourly LST products in order to produce global LST fields. These data are available from the Copernicus Global Land Service in near real time and off-line, covering the GOES disk centred at 75°W and with a spatial resolution of about 4 km at the sub-satellite point. The LST algorithm used for GOES accounts for the fact that the most recent imager on this platform does not have the two split-window channels.

This algorithm, named Dual-Algorithm (DA) [RD-12], consists of two LST algorithms, which are used for day and night-time, respectively. At night a two-channel algorithm is applied, making use of one thermal infrared – around 11 μm – and one middle infrared – around 3.9 μm . During the day a mono-channel algorithm is applied, using the available thermal infrared channel for atmospheric attenuation and surface emissivity. The middle-infrared is discarded for daytime cases to avoid the correction of solar radiation reflected by the surface.

These methodologies are all based on semi-empirical formulations, where LST is expressed as a regression function of TOA brightness temperatures. To minimize LST uncertainties, the algorithms are trained for different classes of satellite view angle, atmosphere water vapour content, and land cover type. However, it is worth mentioning that the Generalized Split-Window algorithm (in place when two TIR channels are available, e.g. SEVIRI, AATSR and MODIS) generally provides lower uncertainty in LST retrievals.

Table 2: Overview information for the GlobTemperature GOES LST products reproduced from [RD-11]

Information	Detail
Product(s) ID	GOES__LST_2
Latest version	1.0
Dataset coverage	01/01/2010 – 31/12/2016
Dataset availability	LST data is available for the entire period of 2010-2014 from the GlobTemperature Data Portal (http://data.globtemperature.info).
Dataset size	~50 Gb / year of data
Geographic coverage	GOES full disk (American continent) every 3 hours and North America hourly
Spatial resolution	0.05° x 0.05° equal angle latitude-longitude grid
Temporal resolution	Hourly (3-hourly before June 20th 2010)
Lead investigator	Isabel Trigo, Instituto Portugues do Mar e da Atmosfera
Contact information	The GlobTemperature Project Team (info@globtemperature.info) Isabel Trigo (isabel.trigo@ipma.pt)
Key dataset strength	Medium resolution instrument (4 km at sub-satellite point); description of LST diurnal cycle (hourly product); LST uncertainty available for the entire period.
Acknowledgement	The hourly LST data derived from GOES and available through the GlobTemperature portal is the LST product used by Copernicus Global Land Service (http://land.copernicus.eu/global/products/lst).
Instrument website	http://www.goes.noaa.gov/goes-e.html http://www.ospo.noaa.gov/Products/land/glst

2.8.2 GlobTemperature MODerate resolution Imaging Spectrometer (MODIS) LST Product

The GlobTemperature Terra-MODIS LST product (MOGSV_LST_2) has been produced from MODIS Collection 6 input data with a formulation independent of the operational Terra-MODIS LST product (MOD11_L2). The subsequent description of this product is taken from the GlobTemperature Product User Guide [RD-11].

The GlobTemperature Terra-MODIS products primarily provide data on LST and its associated uncertainty. It further provides auxiliary information that has been used for the LST retrieval, such as emissivity and quality control flags. A complete set of LST (and accompanying AUX) datafiles is available covering the entire Terra-MODIS mission (a similar product is also available from the Aqua satellite). The temporal resolution of the Level-2 swath data are 5-minute granules consistent with the MODIS operational Level-1b and Level-2 data. All LST data and associated fields are derived from the most recent (Collection 6) data: Level-1b geolocation and viewing geometry (MOD03); Level-1b radiances (MOD021KM); and Level-2 cloud product (MOD35_L2). Latest collections of the MODIS cloud mask include refinements to account for surface elevation in the cloud masking algorithm [RD-13]. Future evolution will involve the adaptation of the ULEIC_V3 restricted Bayesian infrared cloud masking algorithm [AD-4] used for (A)ATSR and being implemented for SLSTR.

The GlobTemperature Level-2 Terra-MODIS LST algorithm (MOGSV_LST_2) uses the generalized split-window (SW) approach [RD-14], similar to the split-window method used for AVHRR data, to estimate LST as a linear function of clear-sky TOA brightness temperatures from bands 31 and 32 centred on 11 μm and 12 μm respectively. Retrieval coefficients are categorised into classes of satellite viewing angle and water vapour.

Land surface emissivity (LSE) is estimated from the CIMSS database of land surface emissivity [RD-15]. This is available at ten wavelengths between 3.6 μm and 14.3 μm , - including emissivity at 10.8 μm and 12.1 μm – at a spatial resolution of 0.05°. It has been derived using the MODIS operational land surface emissivity product and by applying a baseline fit method to fill in the spectral gaps between the six infrared emissivity wavelengths. The dataset is available as monthly filled files from 2003 to 2014 inclusive in netCDF format. Monthly Climatology has been derived for use outside of the available data window. The data itself is spatially and temporally interpolated onto the ~1 km grid for the given day of the satellite acquisition.

The GlobTemperature Terra-MODIS product is a “value-added” dataset in that it provides not only LST, LSE, and accompanying quality control flags, but also full resolution geolocation and viewing geometry data in the GlobTemperature harmonised format. Furthermore a full breakdown of the pixel-level uncertainty budget is provided consistent with the 3-component model used for the GlobTemperature (A)ATSR product.

Table 3: Overview information for the GlobTemperature Terra-MODIS “value-added” LST products made available via the GlobTemperature Data Portal reproduced from [RD-11]

Information	Detail
Product(s) ID	MOGSV_LST_2
Latest version	2.0
Dataset coverage	05/03/2000 – 31/12/2014
Dataset availability	Full resolution Level-2 LST data for the Terra-MODIS mission up to end-2016 are available from the GlobTemperature Data Portal (http://data.globtemperature.info)
Dataset size	~25 Tb
Geographic coverage	Global
Spatial resolution	1 km at nadir
Temporal resolution	16 days repeat cycle, 288 granules per day of 5 minute duration
Lead investigator	Darren Ghent, University of Leicester
Contact information	The GlobTemperature Project Team (info@globtemperature.info) Darren Ghent (djg20@le.ac.uk)
Key dataset strength	Accurate instruments; sub-daily near-global coverage; long time-series; detailed uncertainty budget; full resolution geolocation and viewing geometry
Acknowledgement	The MODerate resolution Imaging Spectroradiometer (MODIS) LST products are made available through the GlobTemperature data portal with the support of the European Space Agency (ESA) and the UK National Centre for Earth Observation (NCEO). MODIS L1B Calibrated Radiances, L1B geolocation and viewing geometry, and L2 cloud masks acquired from the NASA Land Processes Distributed Active Archive Center (LP DAAC), USGS/Earth Resources Observation and Science (EROS) Center, Sioux Falls, South Dakota. 2001
Instrument website	http://modis.gsfc.nasa.gov/
Product heritage	The GlobTemperature “value-added” products MOGSV_LST_2 utilise the generalised split window approach consistent with the MOD11 operational product. Enhancements include: Data in GlobTemperature harmonised Consistent approach to providing full uncertainty breakdown Full resolution geolocation and viewing geometry

2.8.3 GlobTemperature Spinning Enhanced Visible and Infrared Imager (SEVIRI) LST Product

The Spinning Enhanced Visible and Infrared Imager (SEVIRI) is the main sensor onboard Meteosat Second Generation (MSG), a series of 4 geostationary satellites to be operated by EUMETSAT. The GlobTemperature SEVIRI data (SEVIR_LST_2 V1.0) are available in an hourly resolution, which can then be matched-up with in situ data. SEVIR_LST_2 V1.0 data are simply a reformatted and re-projected version of the LSA-SAF product [RD-16; RD-17; RD-18]. A summary of the information for the SEVIR_LST_2 product can be found in [RD-11], a brief summary of which is provided below.

SEVIRI was designed to observe the Earth disk with view zenith angles (SZA) ranging from 0° to 80° at a temporal sampling rate of 15 minutes. SEVIRI's spectral characteristics and accuracy, with 12 channels covering the visible to the infrared, are unique among sensors onboard geostationary platforms. The first MSG satellite was launched in August 2002, and operational observations are available since January 2004. The High Resolution Visible (HRV) channel provides measurements with a 1 km sampling distance at sub-satellite point (SSP); for the remaining channels the spatial resolution is 3 km at SSP. The nominal SSP is located at 0° longitude and therefore the MSG disk covers Africa, most of Europe and part of South America.

Level 1.5 data are disseminated to users after being rectified to 0° longitude, which means the satellite viewing geometry varies slightly with the acquisition time (satellite zenith angles typically differ by less than 0.25° between consecutive observations).

Table 4: Overview information for the GlobTemperature SEVIRI LST products made available via the GlobTemperature Data Portal reproduced from [RD-11]

Information	Detail
Product_ID	SEVIR_LST_2
Latest version	1.0
Dataset coverage	01/01/2007 – 31/12/2016
Dataset availability	Hourly LST data (SEVIR_LST_2 V1.0) is available for the entire period of 2007-2015 from the GlobTemperature Data Portal (http://data.globtemperature.info). Full temporal (15 minute) and spatial resolution data are available from the LSA-SAF website: http://landsaf.ipma.pt
Spatial resolution	0.05° x 0.05° equal angle latitude-longitude grid
Lead investigator	Isabel Trigo, Instituto Portugues do Mar e da Atmosfera
Contact information	The GlobTemperature Project Team (info@globtemperature.info) Isabel Trigo (isabel.trigo@ipma.pt)



Sentinel-3 MPC
S3 Validation Report – SLSTR

Ref.: S3MPC.UOL.VR.029
Issue: 1.0
Date: 30/06/2017
Page: 21

Key data set strength	Medium resolution instrument (3 km at sub-satellite point); description of LST diurnal cycle (hourly product; up to 15 minute); LST uncertainty available from 2008 onwards.
Acknowledgement	The hourly LST data derived from SEVIRI/Meteosat and available through the GlobTemperature portal are entirely based on the LST product generated within the EUMETSAT Satellite Applications Facility on Land Surface Analysis (LSA-SAF product LSA-001).
Instrument website	http://www.eumetsat.int/website/home/Satellites/CurrentSatellites/ http://www.esa.int/esapub/bulletin/bullet111/chapter4_bul111.pdf

3 Results of Category-A Validation

We present the results of the validation of the approximately four months of SL_2_LST data against in situ observations from both the 11 “Gold Standard” sites for which matchups have been generated (Figure 3, Figure 4, and Table 5) and a selection of the most appropriate complementary sites from the USCRN network (Table 6 and Annex II).

In each case, we present the day and night matchups separately since the SLSTR Level-2 LST algorithm has separate biome-dependent coefficients for both day and night, which provides insight into the algorithm performance for these coefficients at each site.

We show the accuracy and precision of the SL_2_LST data at each site for day and night. The terminology here is therefore consistent both with the SLSTR mission requirements for accuracy, and the GCOS 2016 Implementation Plan (GCOS-200) LST requirements in relation to accuracy and precision [RD-10].

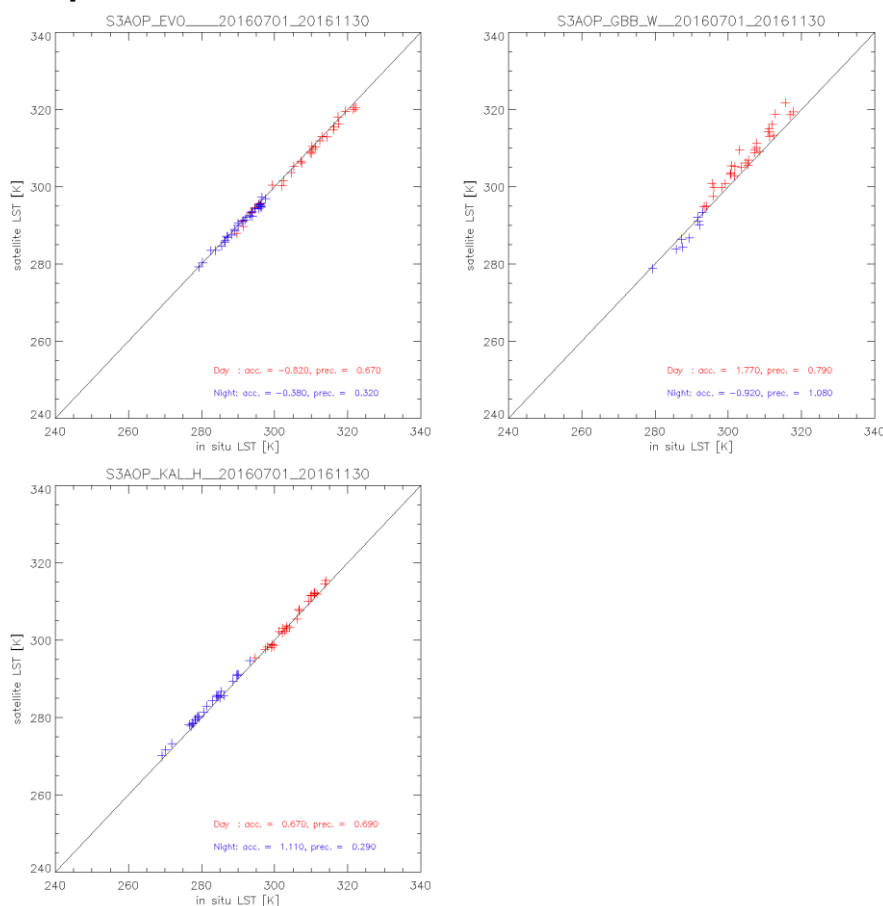
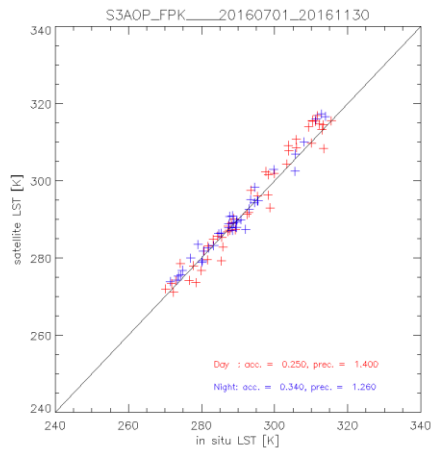
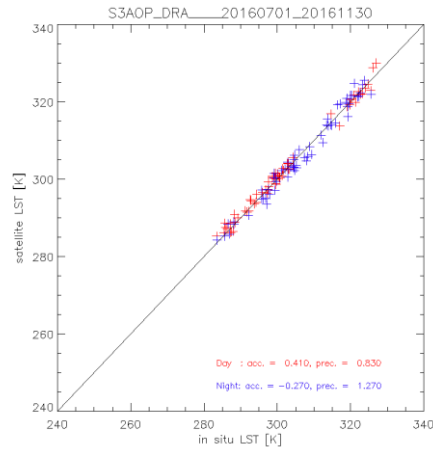
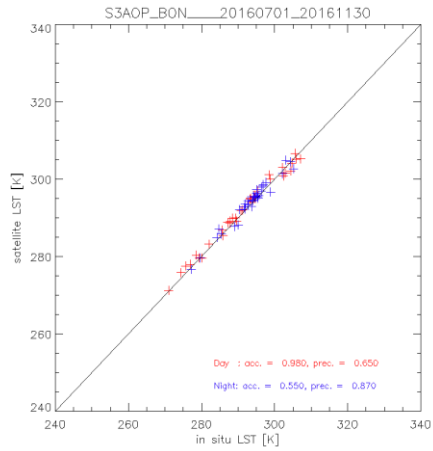


Figure 3: Validation of the SL_2_LST product over the mid-July to mid-November reprocessed period at three Gold Standard in situ stations managed by the Karlsruhe Institute of Technology: Evora, Portugal (left); Gobabeb, Namibia [centre]; Kalahari-Heimat, Namibia (right). [Results courtesy of Maria Martin through the GlobTemperature Project]



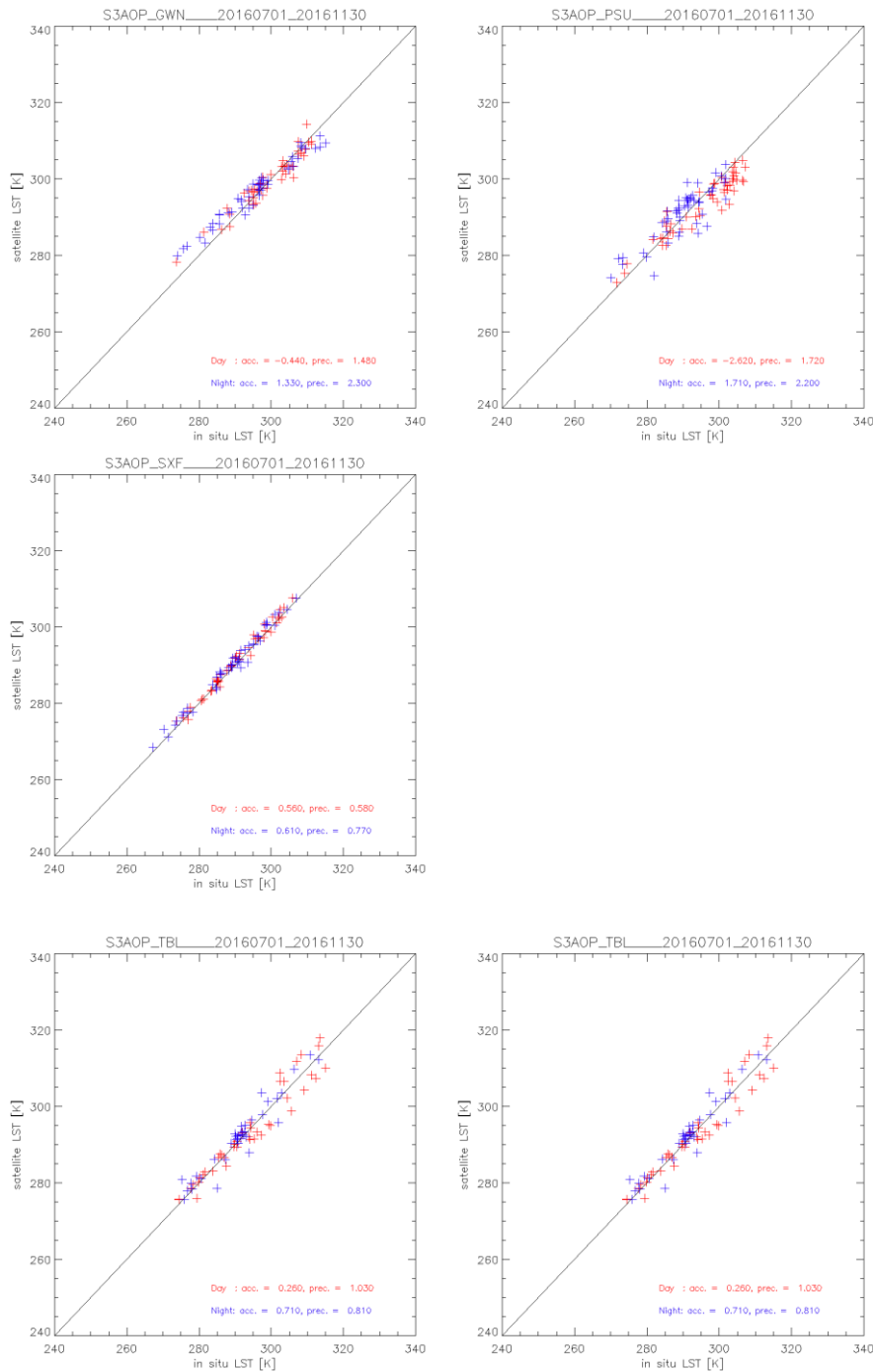


Figure 4: Validation of the SL₂ LST product over the mid-July to mid-November reprocessed period at the seven Gold Standard in situ stations of the SURFRAD network plus a Gold Standard station from the ARM network: Bondville, Illinois top-(left); Desert Rock, Nevada [top-centre]; Fort Peck, Montana (top-right); Goodwin Creek, Mississippi (middle-left); Penn State University, Pennsylvania (middle-centre); Sioux Fall, South Dakota (middle-right); Table Mountain, Colorado (bottom-left); and Southern Great Plains, Oklahoma (bottom-centre).

In the validation against the high-quality stations managed by KIT the accuracy and precision are all ~ 1 K or less (Figure 3 and Table 5). The only notable exception is for the Gobabeb site during the day. A primary source of the larger median difference between SL_2_LST and the in situ observations are the differences at the higher temperatures. This could be due either to the calibration of the thermal channels for high radiances, or the performance of the algorithm at the extremes. For instance, derivation of generic coefficients for bare soil biomes may be regressed to the bulk of the temperature PDF. Moreover, these coefficients are globally robustly, whereas local variation in emissivity within a biome for the same fractional vegetation cover can produce site dependent positive or negative biases.

Further investigation will examine whether there is any correlation between the larger differences and satellite viewing geometry. Furthermore, once more months of data become available a seasonal assessment can be made.

For the validation with respect to the SURFRAD sites and ARM SGP_C1 site (Figure 4 and Table 5) it is evident that while the accuracy is in general very good, the precision is poorer than against the KIT sites. A primary reason for this is the heterogeneity of the surface surrounding the in situ stations. While precision is of secondary priority to accuracy in terms of mission requirements it is important to monitor this over the inter-annual and intra-annual course of the mission to improve upon the upscaling techniques. While the accuracy is generally < 1 K this is not the case at a couple of sites.

At the GWN___ site the night-time difference between SL_2_LST and the in situ observations was larger than during the day. This site is located in rural pasture land in the state of Mississippi, in which the radiometer at the station observes an area of grassland, while the surrounding matrix is dominated by broadleaved deciduous forest. This mixture of grassland and forest in the FOV of the SLSTR pixel cools down slower at night than the grass alone observed by the in situ radiometer, and could explain some of this positive night-time difference.

The PSU___ site shows the largest difference between the SL_2_LST data and the coincident in situ observations. This station is located in a broad Appalachian valley that is very heterogeneous with fields, forests and urban areas surrounding the station. The performance of the SL_2_LST product here is likely to be a result of the differing rates of heating and cooling between the mixture of grass and crops observed by the in situ radiometer and the mosaic of different surface types observed by the SLSTR pixel FOV. Further higher resolution characterisation of this site will be performed during routine validation to maximise the use of this site.

Table 5: Validation of the SL_2_LST product over the mid-July to mid-November reprocessed period at the three Gold Standard in situ stations managed by the Karlsruhe Institute of Technology, and the eight Gold Standard sites of the SURFRAD and ARM networks.

Network	Site Code	Day			Night		
		N	Accuracy	Precision	N	Accuracy	Precision
KIT__	EVO__	30	-0.82	0.67	32	-0.38	0.32
KIT__	GBB_W_	31	1.77	0.79	9	-0.92	1.08
KIT__	KAL_H_	26	0.67	0.69	27	1.11	0.29
SURFD	BON__	34	0.98	0.65	35	0.55	0.87
SURFD	TBL__	53	0.26	1.03	43	0.71	0.81
SURFD	DRA__	67	0.41	0.83	65	-0.27	1.27
SURFD	FPK__	58	0.25	1.40	49	0.34	1.26
SURFD	GWN__	53	-0.44	1.48	53	1.33	2.30
SURFD	PSU__	56	-2.62	1.72	55	1.71	2.20
SURFD	SXF__	52	0.56	0.58	55	0.61	0.77
ARM__	SGP_C1	55	0.17	1.91	54	-0.02	2.10

Validation against the complementary USCRN stations produce a larger number of statistics than the Gold Standard sites alone (Table 6 and Annex II). For many of these the accuracy and precision is < 1 K for both day and night. For some it is > 1 K and in a few cases of the order of 2-3 K. Where the difference is large there is a tendency for this to be the case for both day and night indicating that sub-pixel variability is impacting the usability of the site. A further pre-selection of sites will be performed in which the surface will be better characterised at each site, and if need be a pixel more representative of the FOV of the in situ radiometer near to the site will be used in the matchup. Further investigation will also examine the statistics stratified by biome.

Nevertheless, this broader validation at these USCRN stations provide valuable additional information to the Gold Standard validation. For instance, there are few sites where differences are large and systematic, indicating there are no gross problems with the retrieval for the SL_2_LST product. The spread of the matchups are also in general well within 2 K with an average closer to 1 K.

Table 6: Validation of the SL_2_LST product over the mid-July to mid-November reprocessed period at select USCRN in situ stations.

Site Code	Day			Night		
	N	Accuracy	Precision	N	Accuracy	Precision
ALG19N	52	-0.24	2.55	57	-0.18	1.92
AZE05S	46	-0.50	1.54	50	-0.31	1.16
AZT11W	51	-3.63	0.28	47	-3.63	0.01
AZW35N	57	-0.52	1.01	55	-0.55	0.82
AZY27E	42	-0.68	2.89	65	-1.21	2.08
COC08S	66	2.82	3.42	49	2.91	2.56
COD02E	60	-1.25	2.09	48	-1.83	1.24
COL17W	56	0.18	1.16	44	-0.01	0.88
CON07N	54	-1.27	1.13	51	-1.56	0.84
HIM05N	51	0.75	1.51	49	1.04	1.75
IAD17E	51	0.72	0.66	41	0.72	0.67
IDA17S	61	0.80	1.23	58	1.47	1.03
IDM10W	61	-1.00	1.74	56	-2.68	1.72
ILC09S	42	0.01	0.57	39	0.00	0.72
ILS05N	46	-0.01	0.90	50	0.06	1.15
INB05W	51	-0.29	1.40	45	-0.54	1.53
KSM06S	50	-0.38	1.11	54	-0.64	0.70
KSO19S	57	-0.91	0.97	43	-0.91	0.66
LAL13S	44	-1.01	0.87	39	-1.04	0.54
MEL04N	58	-0.12	2.22	52	-0.74	2.84
MIC01S	51	-2.00	3.52	47	-0.41	3.12
MIG09S	48	-2.99	2.18	48	-1.20	1.79
MOJ24N	52	-0.99	1.10	49	-1.09	0.81
MOS10W	57	-2.08	1.86	47	-0.14	1.82
NDM07E	54	-0.75	1.16	57	-0.49	0.86
NDN05E	46	-0.13	0.64	40	-0.43	0.68



Sentinel-3 MPC
S3 Validation Report – SLSTR

Ref.: S3MPC.UOL.VR.029
 Issue: 1.0
 Date: 30/06/2017
 Page: 28

Site Code	Day			Night		
	N	Accuracy	Precision	N	Accuracy	Precision
NEH20S	57	-2.23	1.06	49	-2.01	1.01
NEL08E	49	1.50	2.24	55	0.56	2.34
NEL11S	52	-1.49	1.36	47	-1.31	1.73
NEW05E	60	-0.44	1.48	54	-0.22	1.84
NML20N	56	-1.83	1.35	36	-2.51	0.80
NMS20N	51	-1.72	2.53	47	-0.09	3.08
NVM03S	62	-1.22	0.97	59	-1.74	1.30
OKG02E	56	-0.76	0.79	47	-0.85	0.69
OKG02S	44	-1.62	0.50	39	-1.44	0.37
OKS02W	55	-1.61	1.07	44	-1.30	0.82
ORR10W	63	-0.12	1.24	55	-0.17	0.80
PAA02N	51	-1.15	1.76	56	-0.41	1.99
SCB03W	52	-2.62	0.91	38	-2.18	1.07
SDA35W	53	-0.81	0.59	53	-1.38	0.74
SDB13E	56	-0.39	1.05	42	-0.77	1.12
SDP24S	60	-1.55	2.16	43	-0.73	1.34
TXM06E	34	-1.76	0.77	28	-2.03	0.57
TXM19S	45	-1.57	0.62	48	-1.74	0.62

4 Results of Category-C Validation

We show the comparison between SL_2_LST and three independent LST products in a global / regional scale: i) SL_2_LST vs. GlobTemperature Terra-MODIS LST; ii) SL_2_LST vs. GlobTemperature GOES LST (GOES__LST_2); and iii) SL_2_LST vs. GlobTemperature SEVIRI LST (SEVIR_LST_2).

Overall differences are generally < 1 K between SL_2_LST and the three independent products. Where the differences are larger they tend to be for biomes where both viewing geometry and gradient of solar heating are significant factors. While no biome stands out as being systematically different across the three intercomparisons, it is notable that the right and left side of the SLSTR swath do produce different results in the comparisons.

While there is no “truth” reference product, these intercomparisons do show whether the LST products are consistent with other. Moreover, the differences between the SL_2_LST product and all three “reference” products are comparable within the uncertainty range of the reference products. Note, a more informative analysis utilising the uncertainties of both products within an intercomparison is not possible until the uncertainty model of SL_2_LST is evolved. The individual comparisons are detailed below.

4.1 SL_2_LST vs. GlobTemperature Terra-MODIS

The local equatorial crossing time of Terra-MODIS is 10:30 and 22:30 compared with 10:00 and 22:00 for SLSTR. However, it is still possible to find matchups where orbits intersect within the ± 7.5 minute temporal threshold, particularly at the high latitudes. Nevertheless, sufficient individual matchups over all latitudes enable a monthly global analysis. Here we show the results for two months of the re-processed data period: August 2016 and September 2016 (Figure 5). Since July and November are only part-months these are omitted from this analysis, while availability of data in October is affected by the decontamination of the SLSTR instrument from 30 September to 6 October 2016.

For both August and September, the daytime differences are small with few notable regions of high differences. Where differences all come from a single matchup between two orbits the potential for temporal differences in the matchups to influence the comparison can increase. The differences at night are generally lower than the day, where the temporal difference between matchups has a weaker influence.

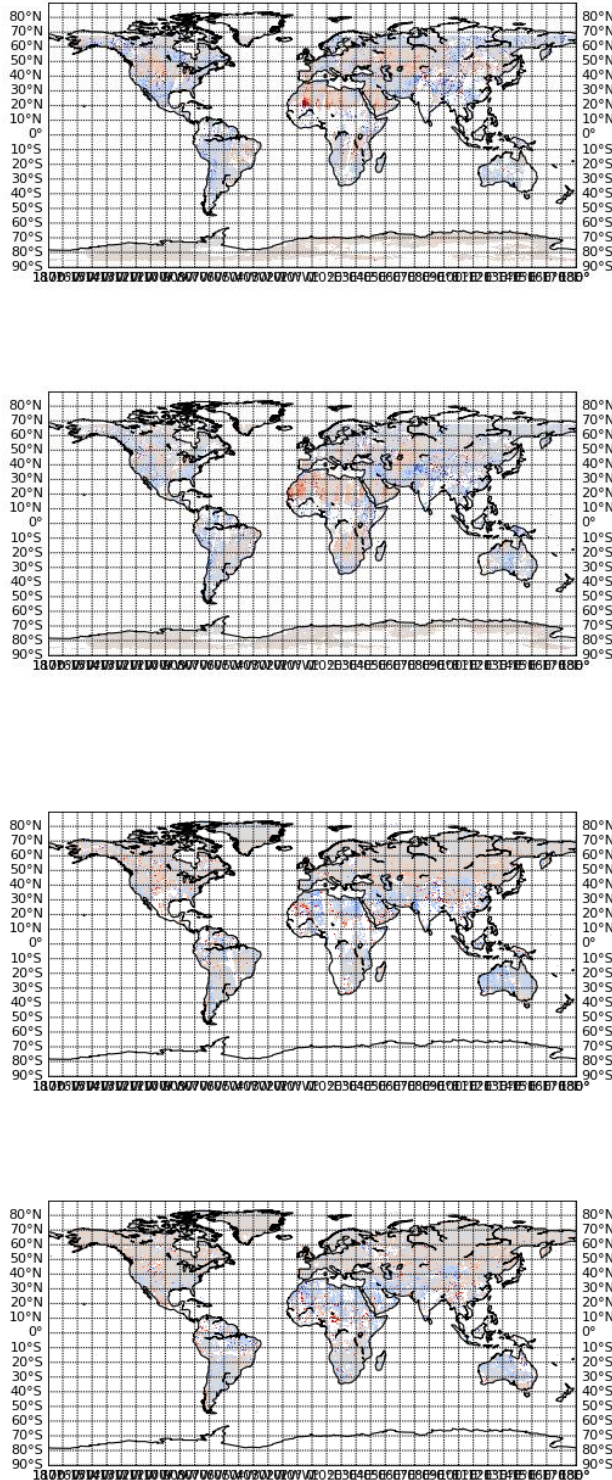
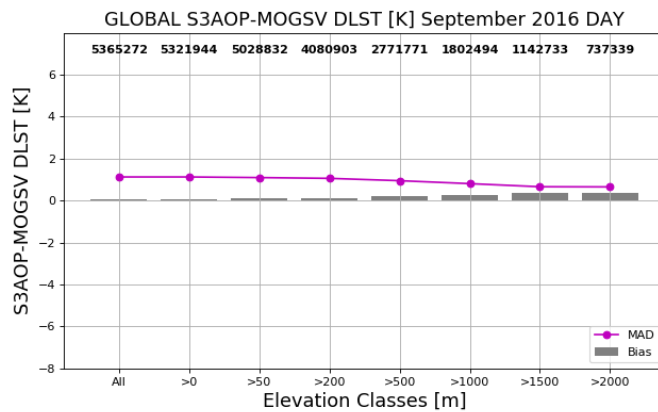
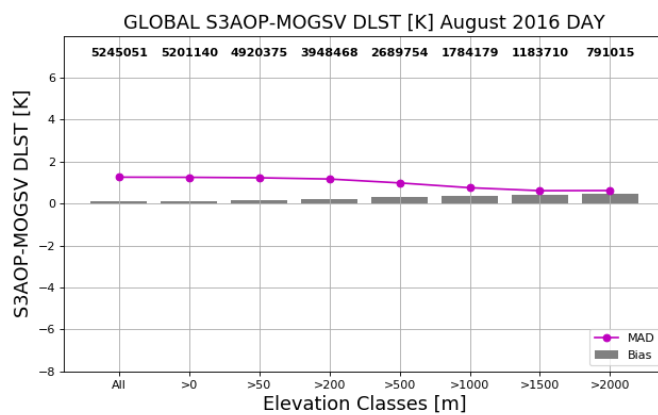


Figure 5: Monthly median Global SNO LST differences between SL_2_LST and GlobTemperature Terra-MODIS for August 2016 (left), September (centre) and October (right). Daytime differences are in the top row and night-time differences in the bottom row.

On a global scale orography appears to have a minimum control over the differences between SL_2_LST and GlobTemperature Terra-MODIS LST, with no elevation class showing differences greater than 0.5 K in any of the compared months – either for day of night (Figure 6). The same is true when comparison is made with respect to the SLSTR land cover classes (biomes) (Figure 7) – in all cases the differences are within 1 K. There are a few biomes (5, 8, 21, 22, 25), where although the differences are below 1 K the difference is approximately the same across the two months – particularly during the day. As such, these biomes will be monitored to assess how systematic this is once other full months are processed; it may indicate a required future fine tuning of these coefficients.



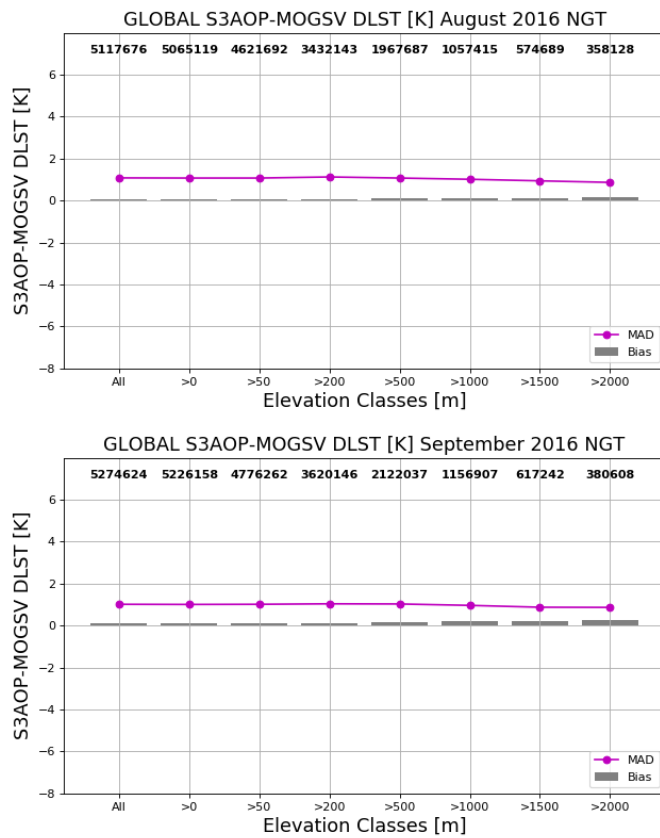


Figure 6: Monthly median (bars) and robust standard deviation (points) Global SNO LST differences between SL_2_LST and GlobTemperature Terra-MODIS with respect to elevation classes for August 2016 (left), September (centre) and October (right). Daytime differences are in the top row and night-time differences in the bottom row.

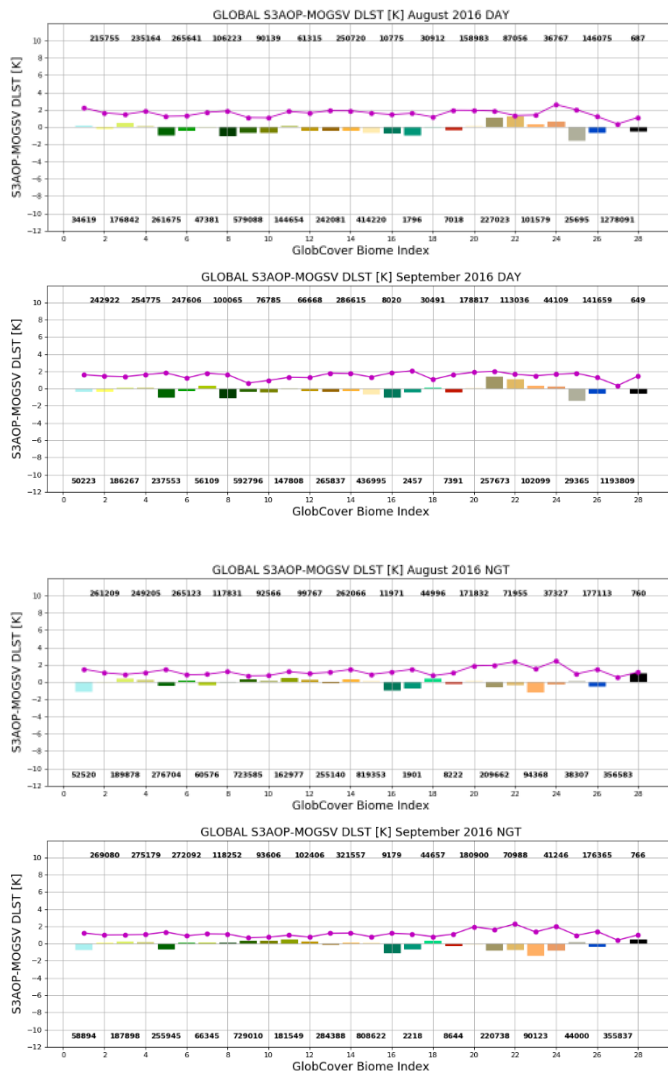


Figure 7: Monthly median (bars) and robust standard deviation (points) Global SNO LST differences between SL_2_LST and GlobTemperature Terra-MODIS with respect to SLSTR land cover classes for August 2016 (left), September (centre) and October (right). Daytime differences are in the top row and night-time differences in the bottom row.

Satellite viewing geometry is also a factor in explaining the differences between the products. Figure 8 shows the difference with respect to the satellite viewing angle of the (non-reference) instrument (SL_2_LST). SLSTR has an asymmetric across-track viewing geometry in the nadir view, with zenith angle ranging between 0 and ~55° to the right of the along-track direction, and between 0 and ~35° to the left of the along-track direction. In the central part of the swath differences between SL_2_LST and GlobTemperature Terra-MODIS LST are small (< 1 K). At the extreme edges of the swath differences become larger, but still < 2 K.

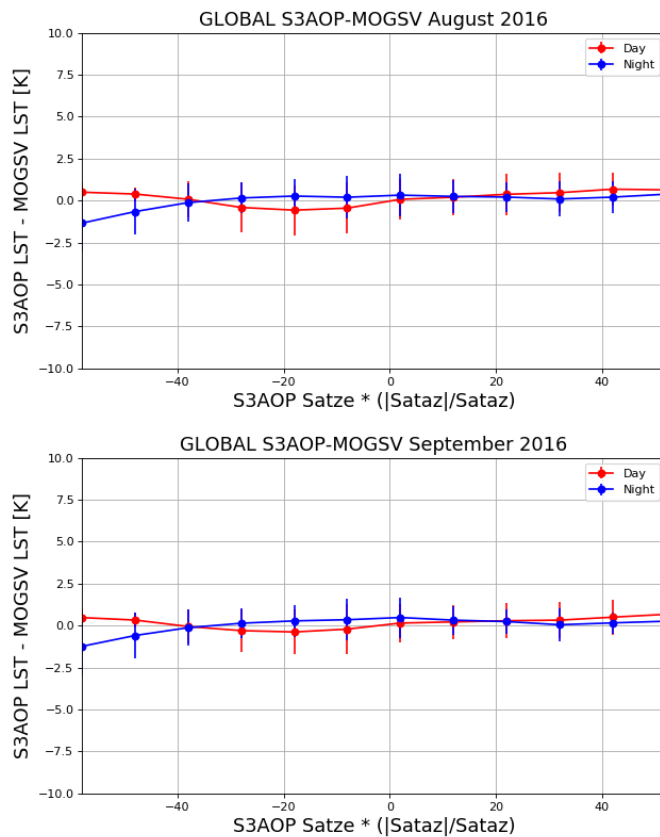


Figure 8: Monthly median Global SNO LST differences between SL_2_LST and GlobTemperature Terra-MODIS with respect to SLSTR viewing geometry for August 2016 (left), September (centre) and October (right). Daytime differences are in red and night-time differences in blue.

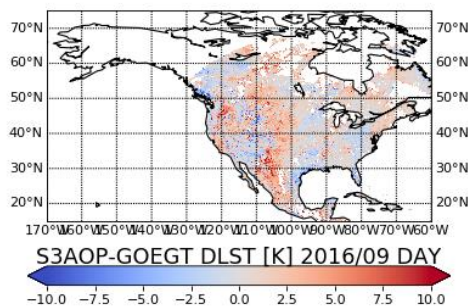
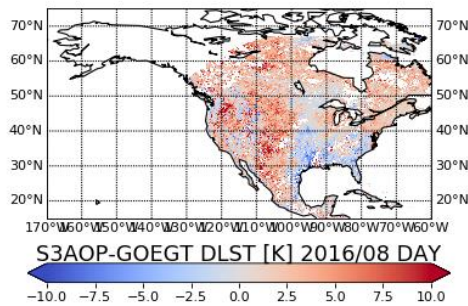
As documented in [AD-1] cloud contamination in the SL_2_LST product remains an area which requires improvement. Nonetheless, the matchups composited on a monthly scale show minimal evidence of excessive cloud contamination.

4.2 SL_2_LST vs. GlobTemperature GOES (GOES__LST_2)

Matchups between SLSTR and GEO data are more common than against LEO data. Here we investigate the differences between SL_2_LST and the GOES__LST_2 product over North America. While this latter is available every hour the individual matching is performed using the acquisition time of each pixel in the GEO disk. Here we show the results for two months of the re-processed data period: August 2016 and September 2016 (Figure 9). As stated previously July, November and October are omitted from this analysis.

Figure 9 shows a consistent pattern of differences for both months, where the mountainous regions of the Rockies have in general a negative difference, with areas of California and the Great Plains showing positive difference. This is more notable in August than September when the mean daytime and night-time temperatures are higher. As with the comparison with respect to GlobTemperature Terra-MODIS, the daytime differences are higher on average than the night-time differences.

Potential cloud contamination, while not excessive, is suggestive during both day and night over a scattering of grid cells: in the Southern States in August during the day, and the Mid-West in August at night for example. Likewise a few very high positive biases in August in the South West may be a result of misses in the GOES cloud masking.



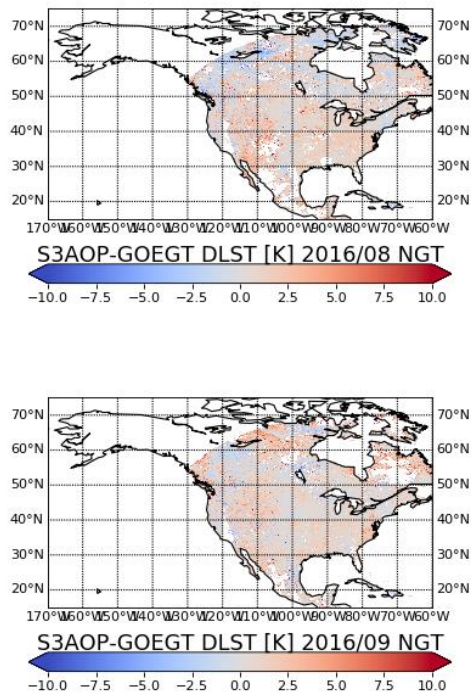


Figure 9: Monthly median SNO LST differences for North America between SL₂_LST and GlobTemperature GOES for August 2016 (left), September (centre) and October (right). Daytime differences are in the top row and night-time differences in the bottom row.

Whilst Figure 10 shows a small change in difference with respect to orography there is still a general increase up to a certain elevation band – this is particularly notable for the robust standard deviation. Change in daytime differences and standard deviations are greater during the day. Daytime differences in orography are expected to be higher than at night since both solar illumination and directional emissivity effects contribute; whereas during local night only directional emissivity effects are a factor.

What is also apparent from Figure 10 is that in each month-diurnal case SL₂_LST is warmer than GOES__LST_2. This difference is < 1 K at night, and between 0.5 K and 1.5 K in September during the day. August daytime positive difference however is in general ~2 K. No evidence though from this intercomparison infers that one product is superior to the other only that they are different (and generally in one direction). This warm-difference during the summer with respect to a GEO product is consistent with other intercomparison exercises [RD-18; RD-27]. A possible cause of this is the spatial anisotropy of LST from different viewing perspectives which is stronger during the day when solar heating occurs.

It must also be noted that while these differences may appear significant the SL₂_LST data still falls within the uncertainty range of the corresponding GOES__LST_2 data, which is of the order of 2 to 3 K both day and night (Figure 11). So from a validation perspective the two products are comparable within the derived uncertainty range.

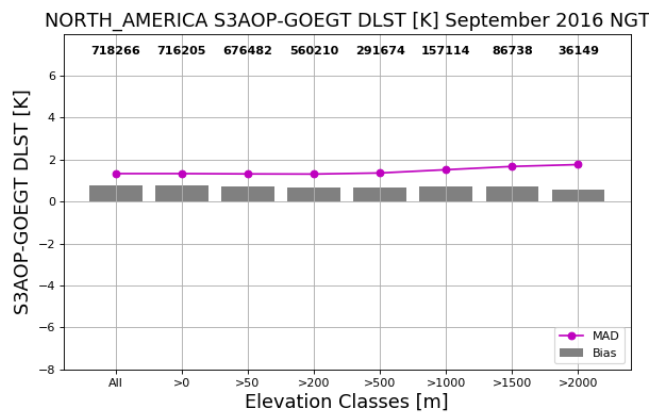
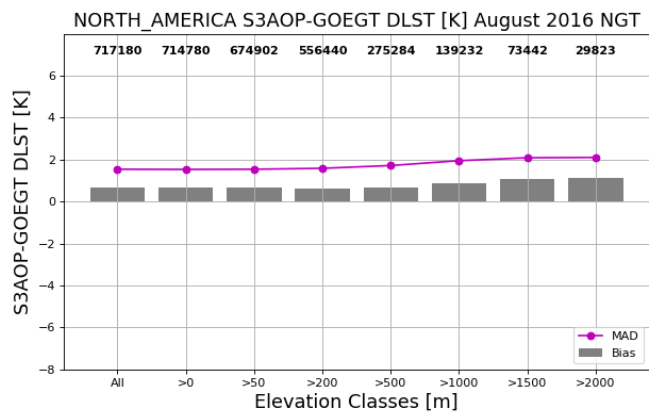
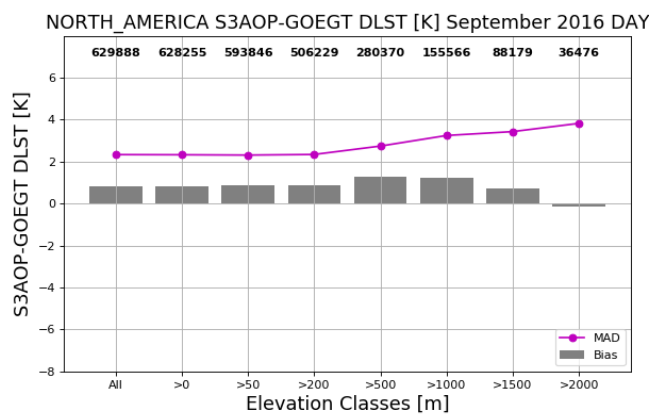
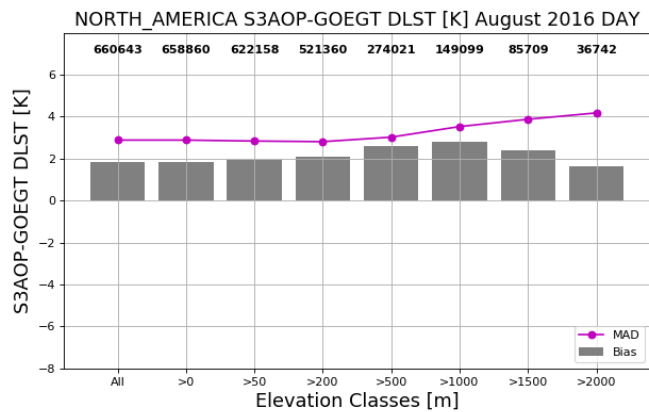
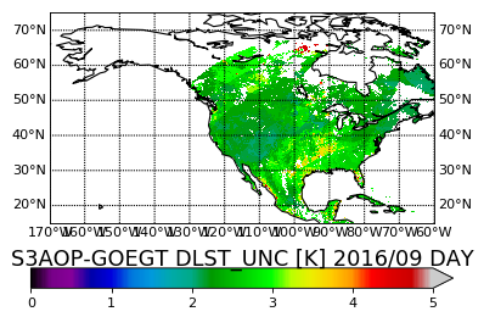
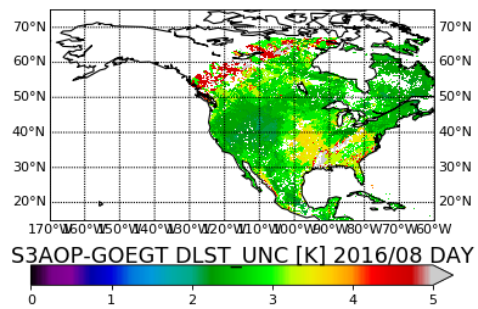


Figure 10: Monthly median (bars) and robust standard deviation (points) SNO LST differences for North America between SL_2_LST and GlobTemperature GOES with respect to elevation classes for August 2016 (left), September (centre) and October (right). Daytime differences are in the top row and night-time differences in the bottom row.



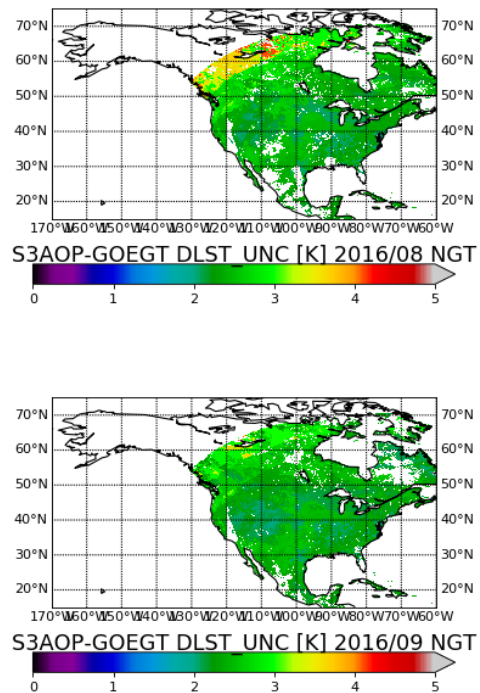


Figure 11: Monthly median LST uncertainties for North America from GlobTemperature GOES for August 2016 (left), September (right). Daytime uncertainties are in the top row and night-time uncertainties in the bottom row.

The intercomparison with respect to land cover metric indicates a consistent pattern of differences across the SLSTR land cover classes (biomes) (Figure 12). The highest differences are found in the mixed vegetation and shrubland classes where different viewing geometries have a greater impact on the respective LSTs. This is seen for both months during the day. There are a few classes which show much larger differences: biomes 18, 23 and 25. The number of matchups for these though are too few for robust statistics to be determined. The night-time difference show little variation as a function of land cover.

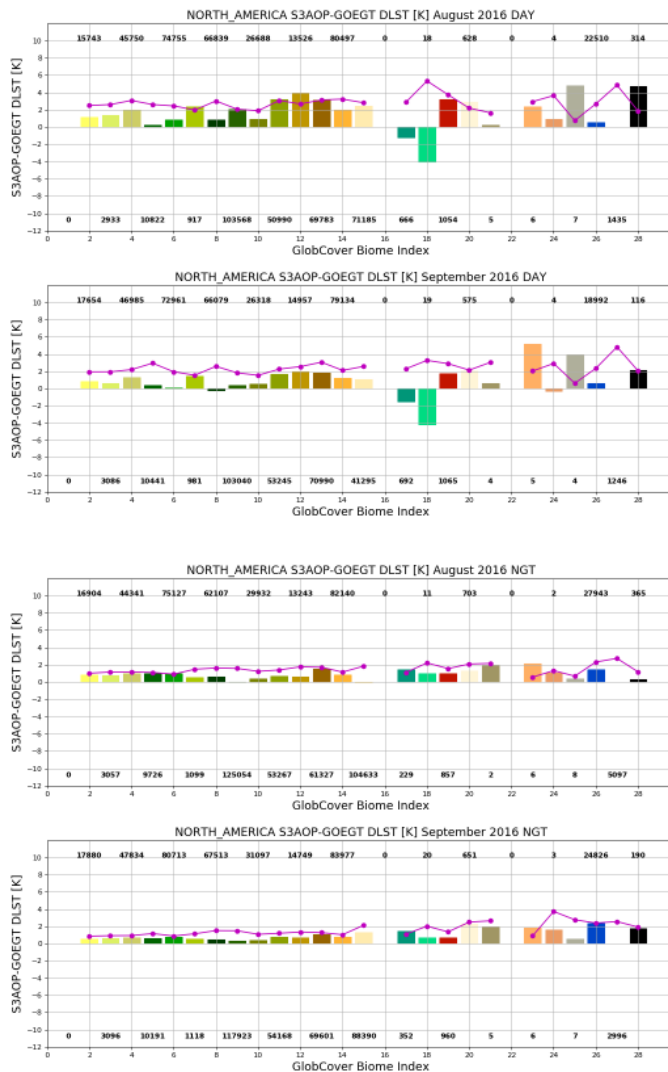


Figure 12: Monthly median (bars) and robust standard deviation (points) SNO LST differences for North America between SL_2_LST and GlobTemperature GOES with respect to SLSTR land cover classes for August 2016 (left), September (centre) and October (right). Daytime differences are in the top row and night-time differences in the bottom row.

The analysis with respect to satellite zenith angle of SLSTR is also informative in determining a potential cause in the systematic difference between SL_2_LST and GOES__LST_2. Figure 13 shows the night-time difference to vary little with viewing angle, whereas in both months a distinct pattern emerges during the day. The daytime difference is close to zero for matchups where the SLSTR data is acquired from the right side of the swath in the along-track direction. The overall positive difference observed between SL_2_LST and GOES__LST_2 during the day does appear to be dominated by differences in matchups using SLSTR data from the left side of the swath.

The SLSTR LST algorithm corrects for across-track differences through parameterisation, and both sides of the nadir swath have this same parameterisation. Instead, it is likely that the differences in the left side are due to the fraction of sunlit and shadow area seen by the respective instruments during local solar morning as a result of their different viewing geometries.

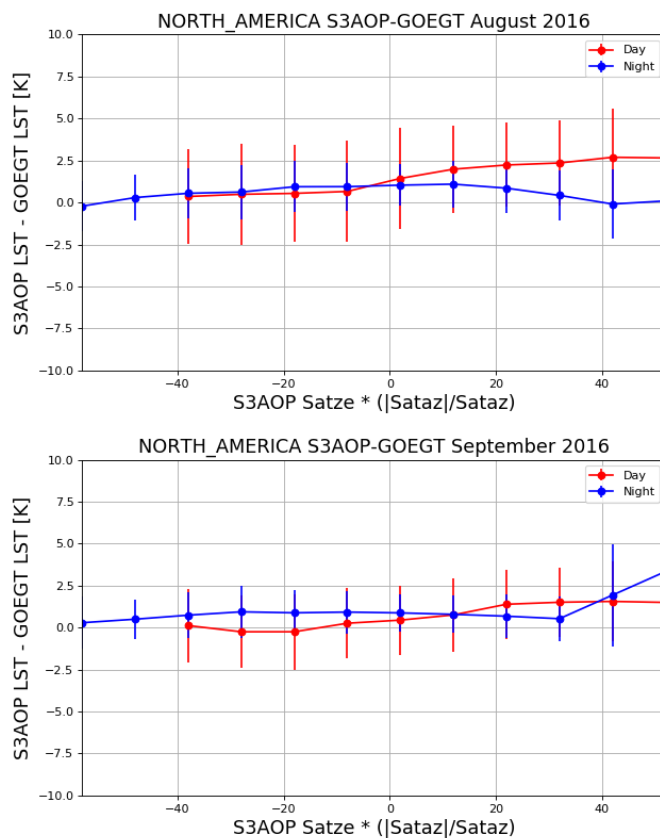


Figure 13: Monthly median SNO LST differences for North America between SL₂_LST and GlobTemperature GOES with respect to SLSTR viewing geometry for August 2016 (left), September (centre) and October (right). Daytime differences are in red and night-time differences in blue.

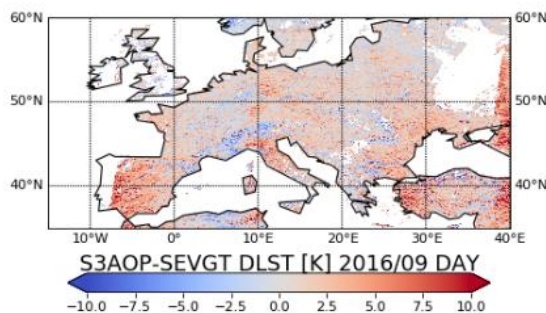
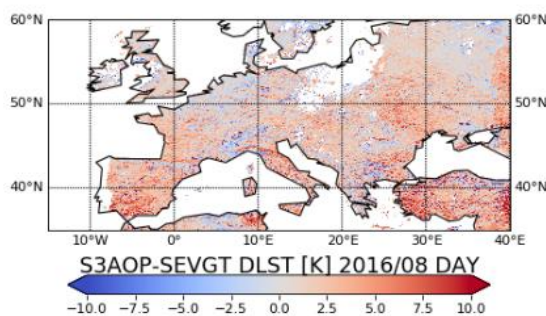
4.3 SL₂_LST vs. GlobTemperature SEVIRI (SEVIR_LST_2)

In addition to intercomparison with respect to GOES_LST_2 we also investigate the differences between SL₂_LST and the SEVIR_LST_2 LST product over Europe. The SEVIRI data is available every

hour, but the individual matching are performed using the acquisition time of each pixel in the GEO disk. Here we show the results for two months of the re-processed data period: August 2016 and September 2016 (Figure 14). As stated previously July, November and October are omitted from this analysis.

There is a consistent pattern of differences for both months sub-divided by day and night. The elevated regions (such as the Alps and Carpathians) have in general a negative difference, whereas much of the rest of the continent shows positive difference, particularly during the day. This is stronger in August than September when the mean daytime and night-time temperatures are higher.

Substantial cloud contamination is not widespread, although some small scale strong negative and positive differences indicate possible misses in the cloud masking of both the respective products.



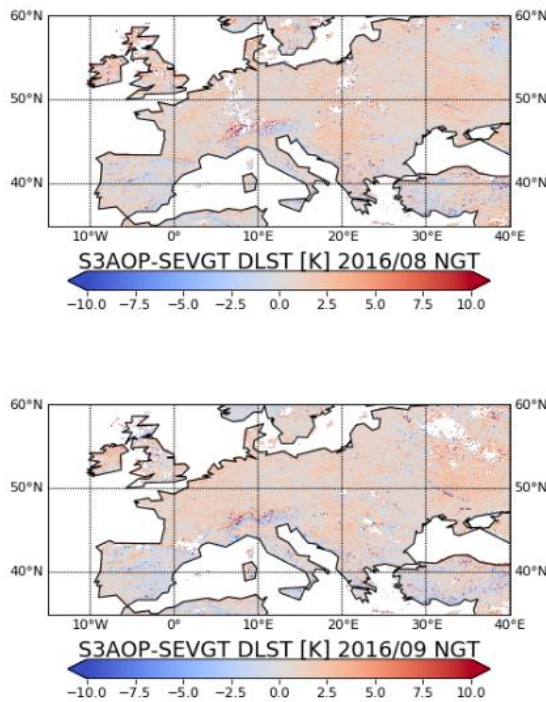


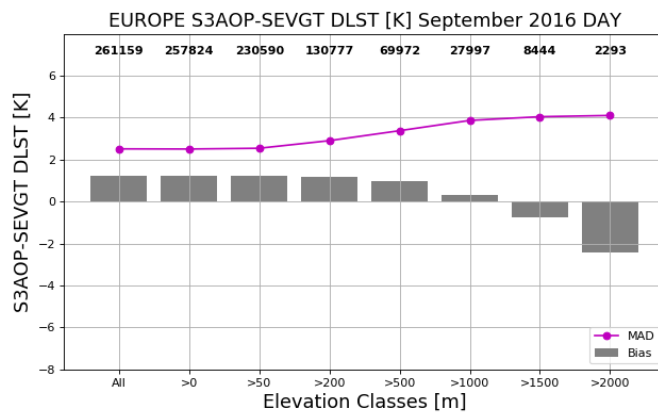
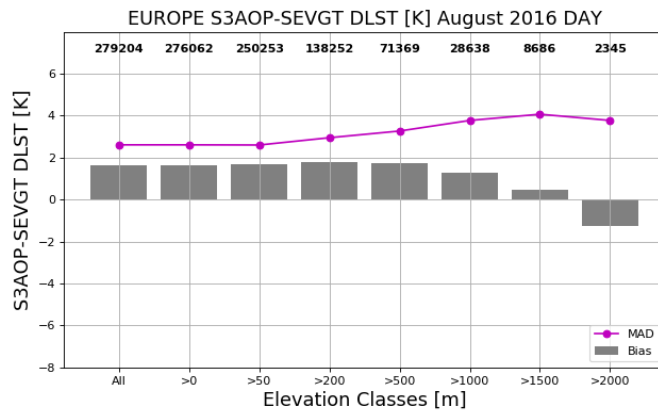
Figure 14: Monthly median SNO LST differences for Europe between SL_2_LST and GlobTemperature SEVIRI for August 2016 (left), September (centre) and October (right). Daytime differences are in the top row and night-time differences in the bottom row.

Unlike for the GOES comparison there is a strong trend in differences with respect to orography (Figure 15). For very high elevation bins both the daytime and night-time differences switch from positive to negative and become increasingly negative towards the highest elevation bin. The robust standard deviation also increase with increasing elevation. The viewing geometry of GOES over North America and SEVIRI over Europe is different meaning the amount of sunlit and shadow fractions of a pixel are not the same, and are likely to be the main reason for the differing responses in the SLSTR LST vs. GEO differences with respect to orography.

At night the differences are < 1 K apart from the very high elevations, whereas the daytime differences are > 1 K (greater in August than September) suggesting the differences may be a function of temperature. This will be investigated further as more full months of data become available. No evidence though from this intercomparison infers that one product is superior to the other only that they are different. At low to mid elevations the warm-difference during the summer with respect to a GEO product is consistent with the comparison against GOES_LST_2 and other intercomparison exercises [RD-18; RD-27].

As with the comparison with respect to GOES_LST_2, it should be understood here also that while these differences may appear significant the SL_2_LST data still falls within the uncertainty range of the

corresponding GlobTemperature SEVIRI LST data, which is of the order of 2 to 3 K both day and night (Figure 16). So from a validation perspective the two products are comparable within the derived uncertainty range.



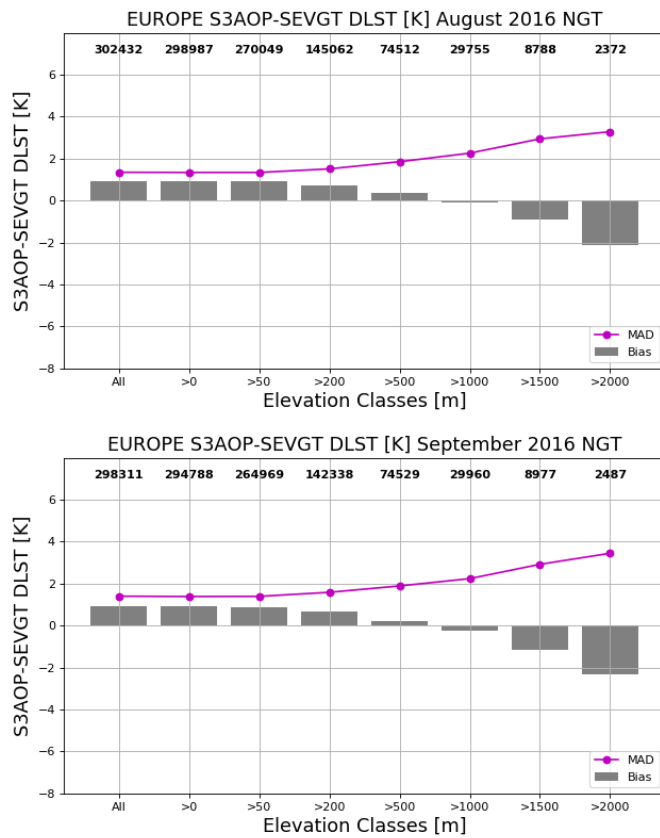


Figure 15: Monthly median (bars) and robust standard deviation (points) SNO LST differences for Europe between SL_2_LST and GlobTemperature SEVIRI with respect to elevation classes for August 2016 (left), September (centre) and October (right). Daytime differences are in the top row and night-time differences in the bottom row.

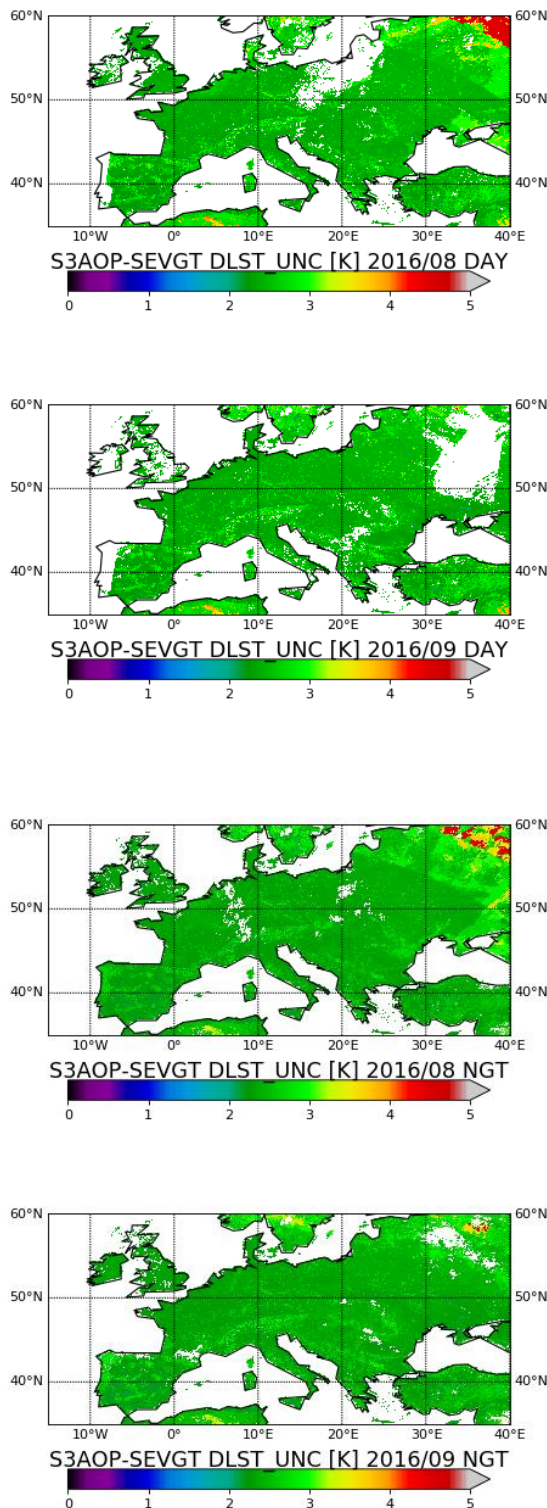


Figure 16: Monthly median LST uncertainties for Europe from GlobTemperature SEVIRI for August 2016 (left), September (right). Daytime uncertainties are in the top row and night-time uncertainties in the bottom row.

The intercomparison with respect to land cover metric indicates a consistent pattern of differences between the two months, but the amplitude of these differences changes by SLSTR land cover class (biome) (Figure 17). The highest differences are found for shrubland, cropland, bare soil, and urban biomes where both different viewing geometries and temporal matchup differences in these surfaces which experience high solar insolation may impact the LST differences. This is much greater during the day supporting this hypothesis. The large negative difference for biome 25 is likely to be influenced by the lack of matchups thus reducing the robustness of the statistics.

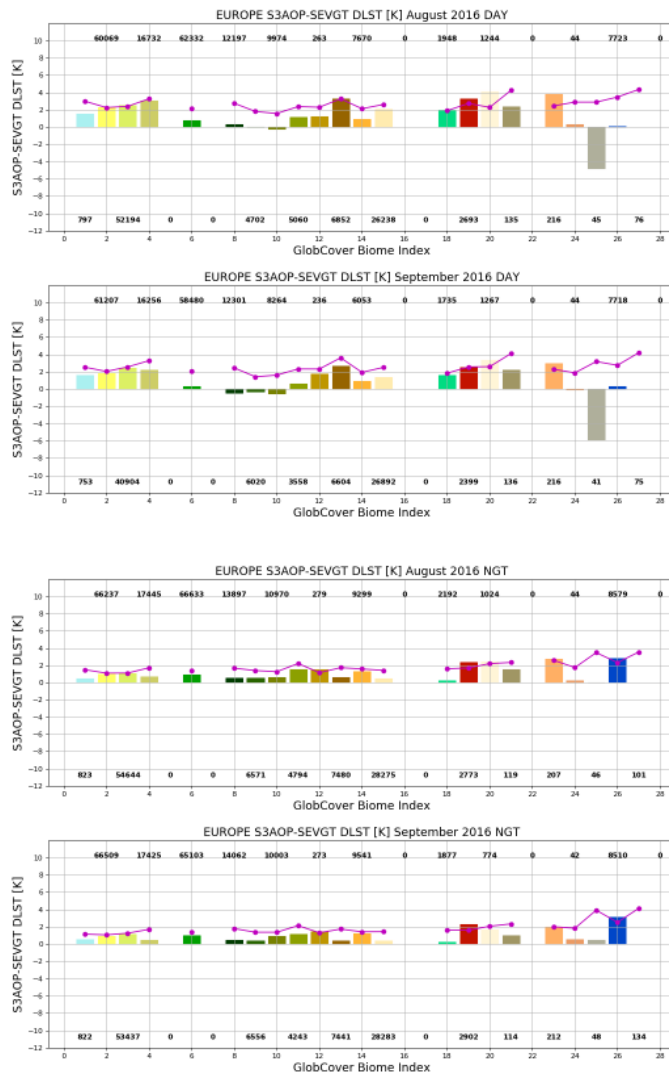


Figure 17: Monthly median (bars) and robust standard deviation (points) SNO LST differences for Europe between SL₂_LST and GlobTemperature SEVIRI with respect to SLSTR land cover classes for August 2016 (left), September (centre) and October (right). Daytime differences are in the top row and night-time differences in the bottom row.

Investigating the differences between SL_2_LST and SEVIR_LST_2 as a function of satellite zenith angle of SLSTR produces further insights. Figure 18 shows little difference between the daytime and night-time differences for most of the SLSTR nadir swath, being between ~0 K and ~1 K. As the satellite zenith angle increases above ~20° on the left side of the swath the overall positive difference observed between SL_2_LST and SEVIR_LST_2 during the day does increase to at least 2.5 K. This is similar to comparison against GOES_LST_2 and is likely due to the fraction of sunlit and shadow area seen by the respective instruments during local solar morning as a result of their different viewing geometries.

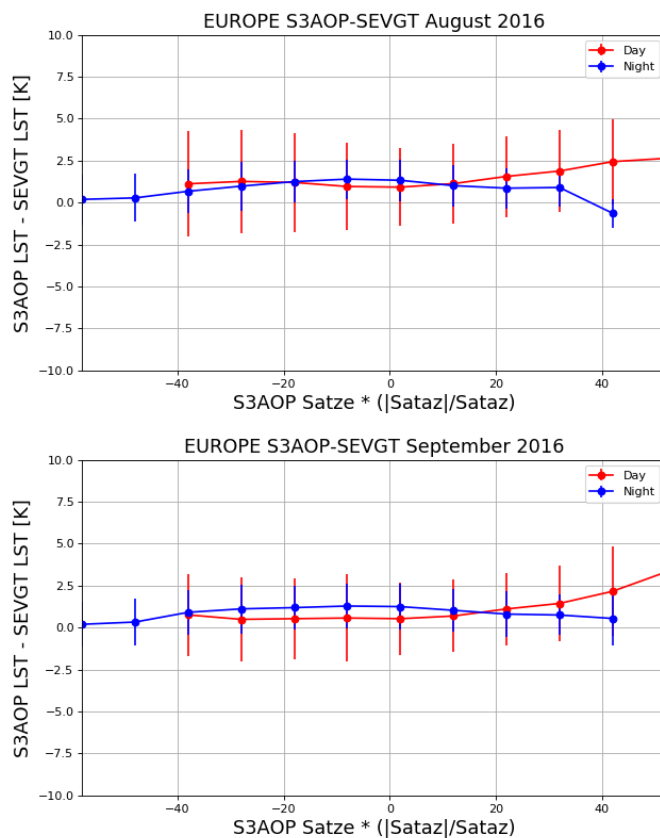


Figure 18: Monthly median SNO LST differences for Europe between SL_2_LST and GlobTemperature SEVIRI with respect to SLSTR viewing geometry for August 2016 (left), September (centre) and October (right). Daytime differences are in red and night-time differences in blue.

5 Conclusions and Recommendations

The results of the validation of SL_2_LST against in situ observations (Category-A) and intercomparison with respect to LEO and GEO reference products (Category-C) can be summarised thus:

5.1 Category-A Validation

Average absolute accuracy (vs. Gold Standard):

- ❖ Daytime: 0.81K
- ❖ Night-time: 1.07K

This daytime accuracy meets the mission requirement (S3-MR-420) of < 1 K. The night-time accuracy is very close to this mission requirement. This also is in line with the GCOS climate requirements of 1 K accuracy [RD-10].

Average precision (vs. Gold Standard):

- ❖ Daytime: 0.72K
- ❖ Night-time: 1.21K

While there is no Sentinel-3 mission requirement for precision, the daytime precision meets the GCOS climate requirement of 1 K [RD-10]. The night-time accuracy is also very close to this climate requirement.

In both cases of accuracy and precision the night-time statistics are affected by the results from the PSU__SURFRAD station which is subject to high surface heterogeneity. Further investigation on the upscaling will be performed to better assess the use of this station for primary validation.

For the USCRN stations the average accuracy is 1.19 K during the day and 1.15 K at night. While these provide lower quality validation they do show that no gross differences are found in the SL_2_LST product, and the accuracy is still very close to the mission requirements (S3-MR-420).

5.2 Category-C Validation

Daytime intercomparison differences are: ~1 K vs. GOES__LST_2 over North America; ~1 K vs. SEVIR_LST_2 over Europe; and < 1 K vs. MOGSV_LST_2 on a Global basis.

Night-time intercomparison differences are: <1 K vs. GOES__LST_2 over North America; <1 K vs. SEVIR_LST_2 over Europe; and < 1 K vs. MOGSV_LST_2 on a Global basis.

Differences with respect to biomes tend to be larger during the day for surfaces with more heterogeneity and/or higher solar insolation. With respect to SLSTR zenith viewing angle differences are larger in the day on the left side of the SLSTR swath in the along-track direction.

5.3 Recommendations

The results of the validation (Category-A) against in situ observations from “Gold Standard” stations show the SL_2_LST product with a accuracy for all matchups of 0.94 K is meeting the overall mission requirement (S3-MR-420) of < 1 K. Intercomparison (Category-C) with respect to other reference products show differences are around 1 K overall. Although this differs by region and reference product, nevertheless all comparisons are within the uncertainty range when considering the uncertainties from the reference products.

Thus the recommendation is to approve the operational release of the Level-2 SL_2_LST product.

There are however some recommendations for further algorithm improvement and product assessment:

- ❖ Further fine-tuning of LST coefficients once we have assessment of full seasonal variability
- ❖ Implementation of a more robust LST uncertainty model for the SL_2_LST product to better quantify the validation and intercomparison
- ❖ Investigation of the algorithm performance and coefficients at high viewing angles on the left side of the SLSTR swath in the along-track direction.

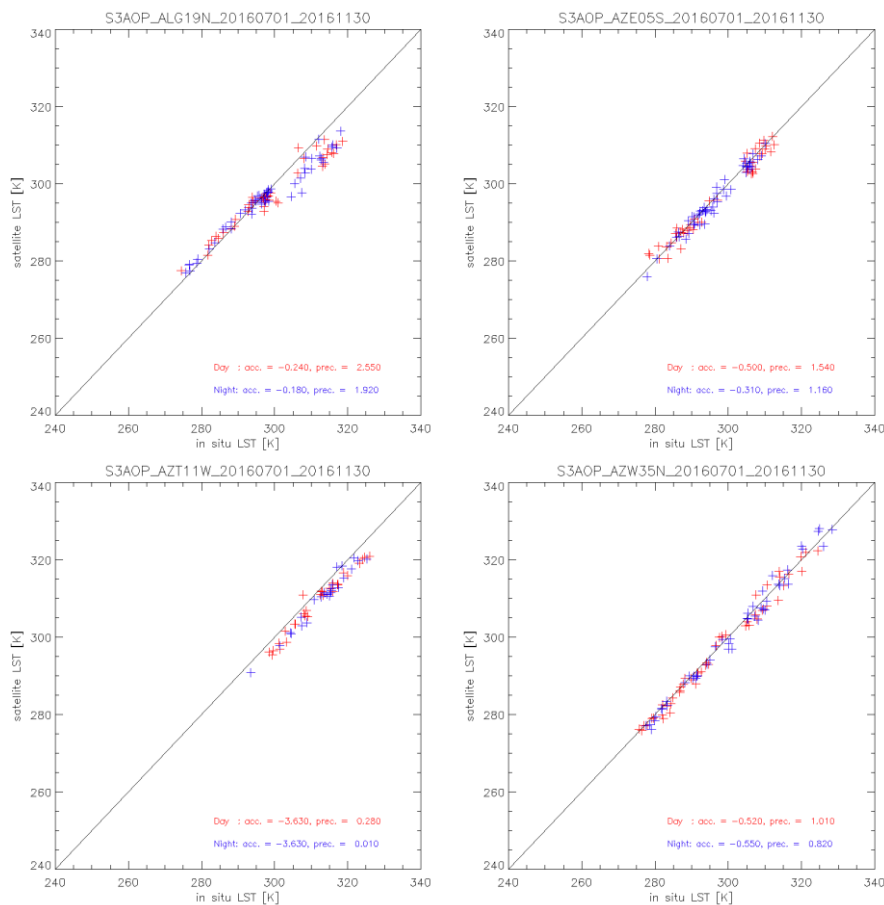
6 Annexes

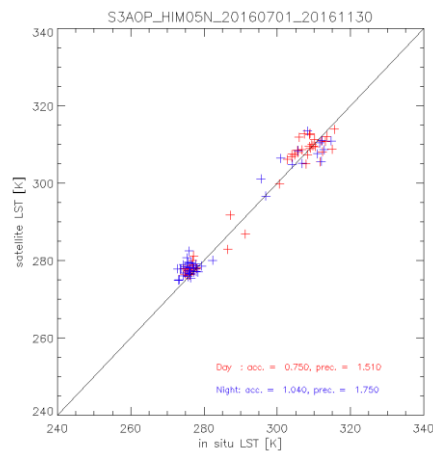
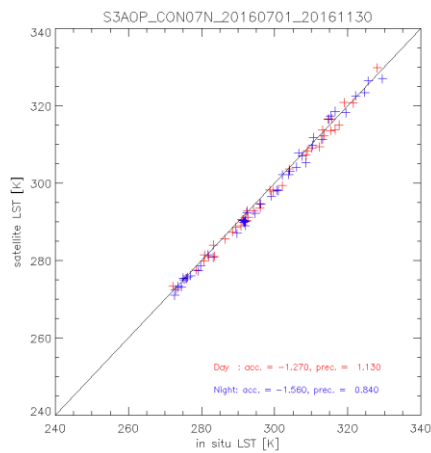
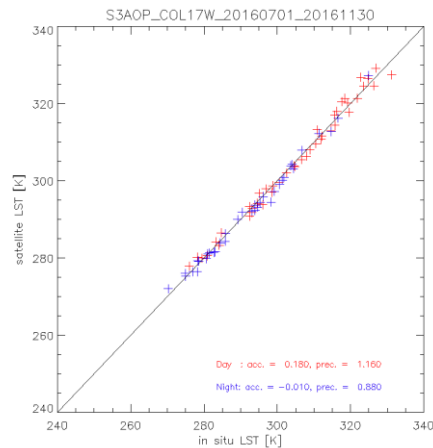
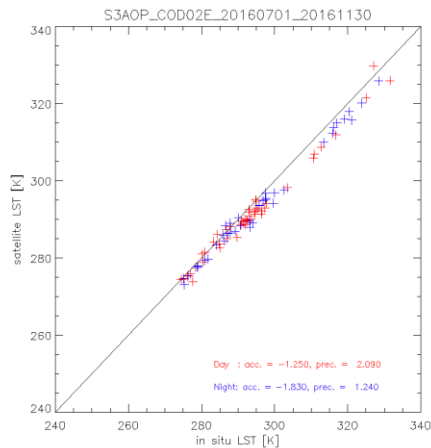
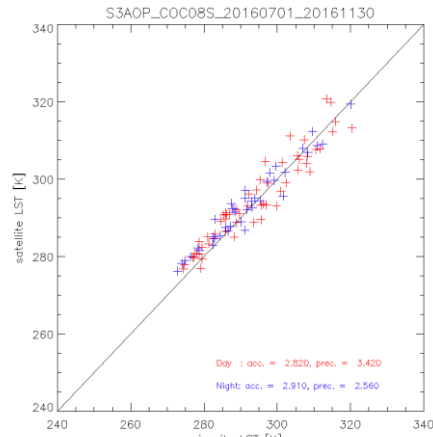
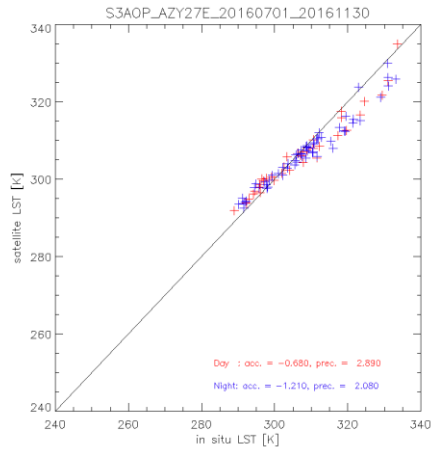
6.1 Annex I: SLSTR Biome Classes

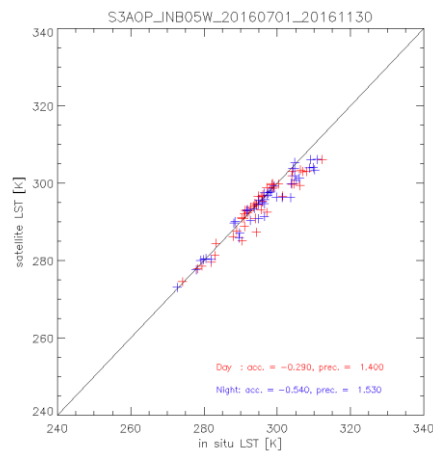
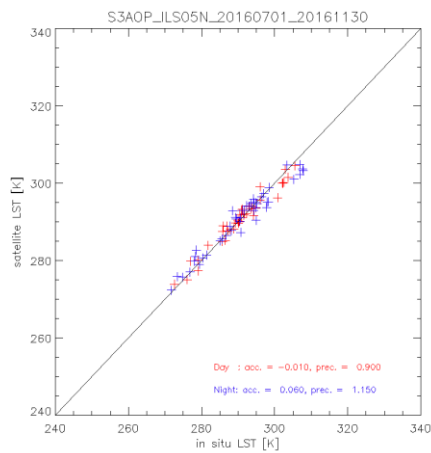
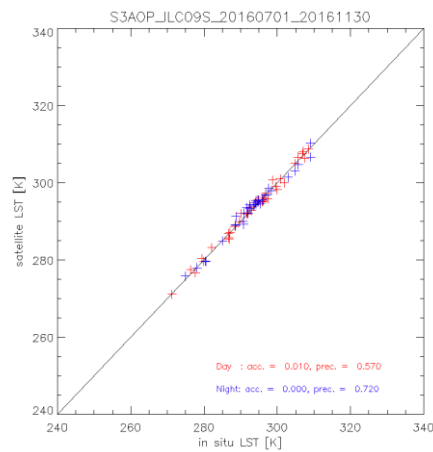
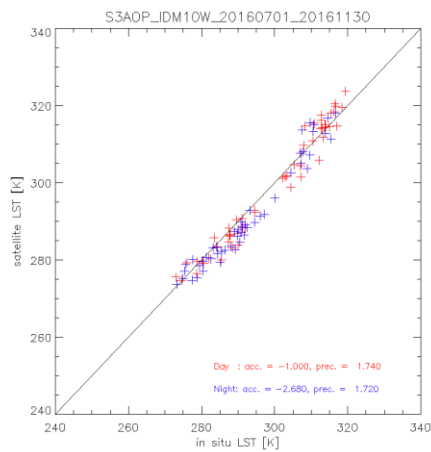
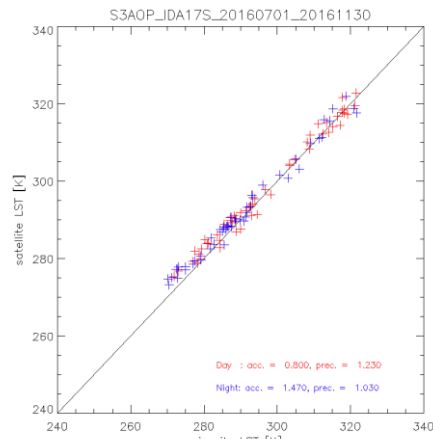
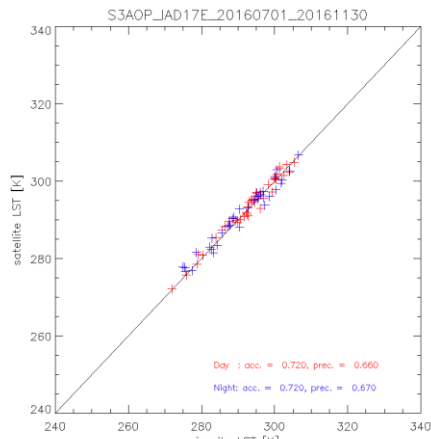
No.	Legend	Based on
0	Water bodies of sea (>10km away from coast)	GC210 (GC0)
1	Post-flooding or irrigated croplands	GC11
2	Rainfed croplands	GC14
3	Mosaic Cropland (50-70%) / Vegetation (grassland, shrubland, forest) (20-50%)	GC20
4	Mosaic Vegetation (grassland, shrubland, forest) (50-70%) / Cropland (20-50%)	GC30
5	Closed to open (>15%) broadleaved evergreen and/or semi-deciduous forest (>5m)	GC40
6	Closed (>40%) broadleaved deciduous forest (>5m)	GC50
7	Open (15-40%) broadleaved deciduous forest (>5m)	GC60
8	Closed (>40%) needleleaved evergreen forest (>5m)	GC70
9	Open (15-40%) needleleaved deciduous or evergreen forest (>5m)	GC90
10	Closed to open (>15%) mixed broadleaved and needleleaved forest (>5m)	GC100
11	Mosaic Forest/Shrubland (50-70%) / Grassland (20-50%)	GC110
12	Mosaic Grassland (50-70%) / Forest/Shrubland (20-50%)	GC120
13	Closed to open (>15%) shrubland (<5m)	GC130
14	Closed to open (>15%) grassland	GC140
15	Sparse (>15%) vegetation (woody vegetation, shrubs, grassland)	GC150
16	Closed (>40%) broadleaved forest regularly flooded - Fresh water	GC160
17	Closed (>40%) broadleaved semi-deciduous and/or evergreen forest regularly flooded - Saline water	GC170
18	Closed to open (>15%) vegetation (grassland, shrubland, woody vegetation) on regularly flooded or waterlogged soil - Fresh, brackish or saline water	GC180
19	Artificial surfaces and associated areas (urban areas >50%)	GC190
20	Bare areas of soil types not contained in biomes 21 – 25	GC200 and other USDA soil types
21	Bare areas of soil type “Entisols – Orthents”	GC200 / USDA-99
22	Bare areas of soil type “Shifting sand”	GC200 / USDA-1

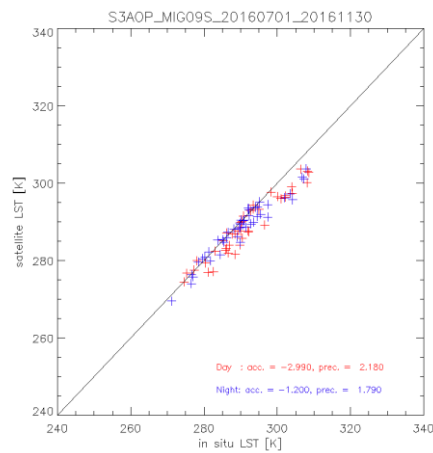
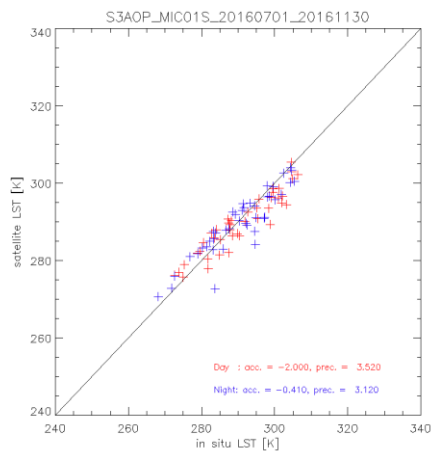
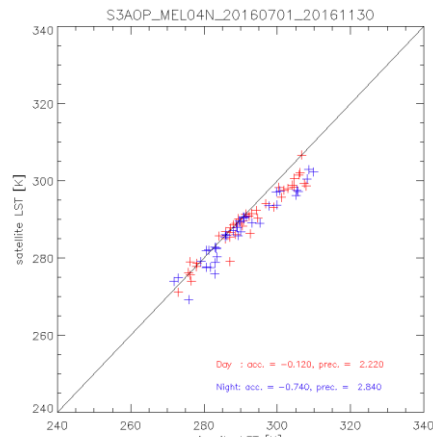
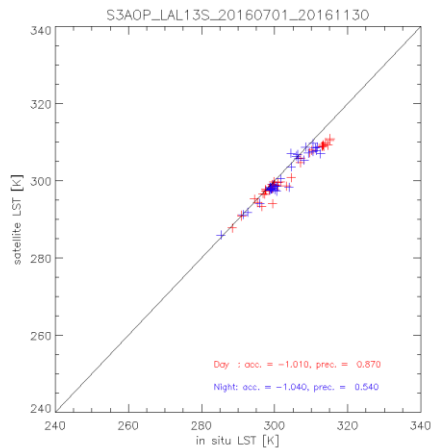
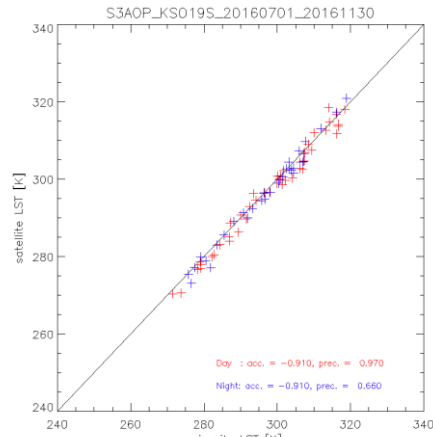
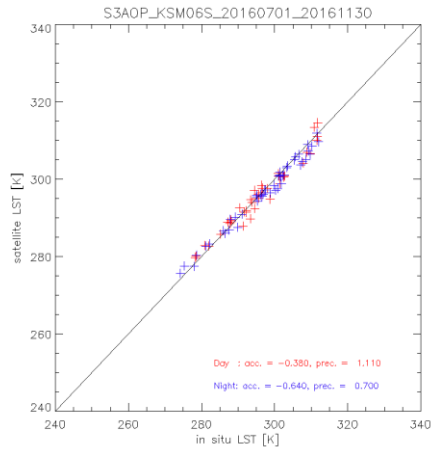
No.	Legend	Based on
23	Bare areas of soil type "Aridisols - Calcids"	GC200 / USDA-55
24	Bare areas of soil type "Aridisols - Cambids"	GC200 / USDA-56
25	Bare areas of soil type "Gelisol - Orthels"	GC200 / USDA-7
26	Water bodies (inland lakes, rivers, sea: max 10km away from coast)	GC210
27	Permanent snow and ice	GC220
28	No data (burnt areas, clouds, etc)	GC230

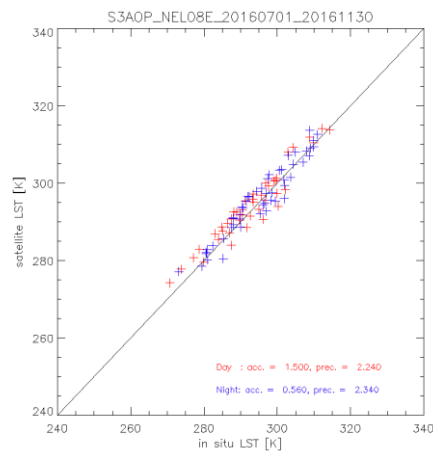
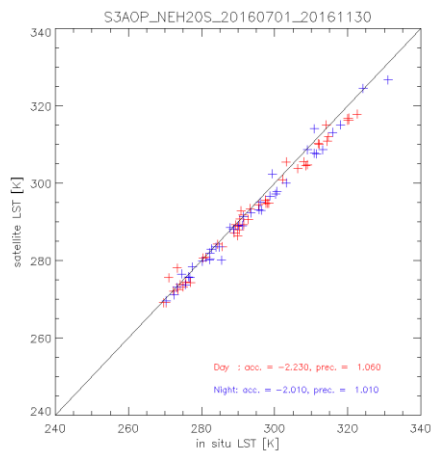
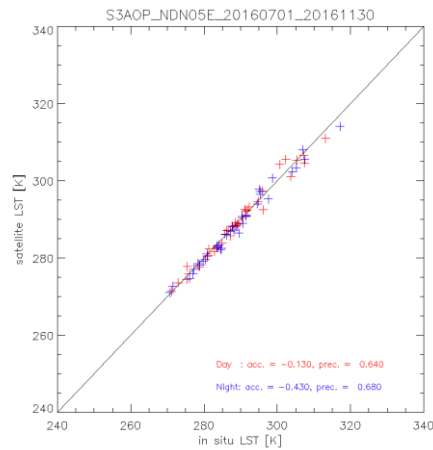
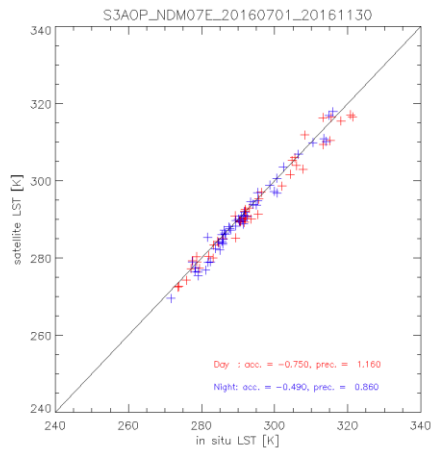
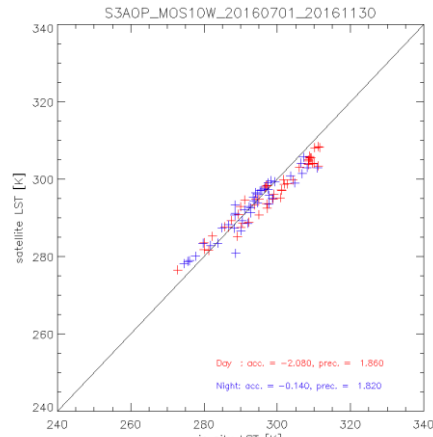
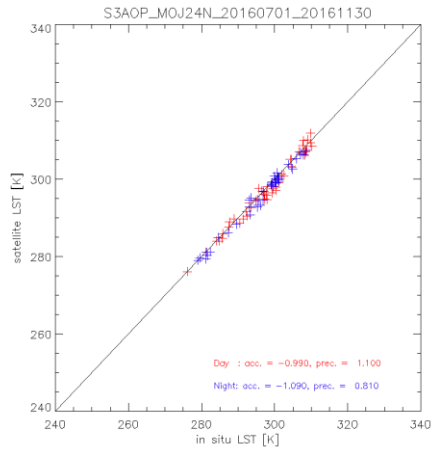
6.2 Annex II: USCRN Validation Plots

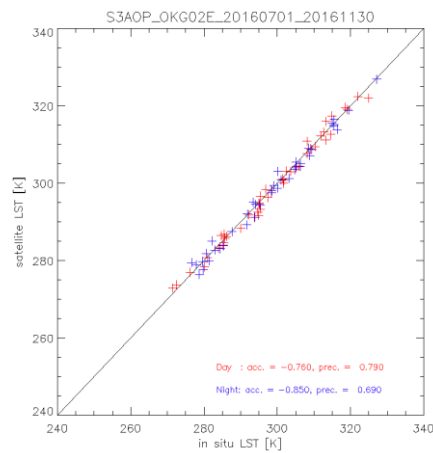
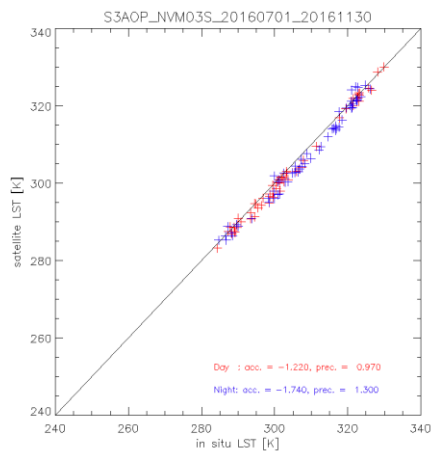
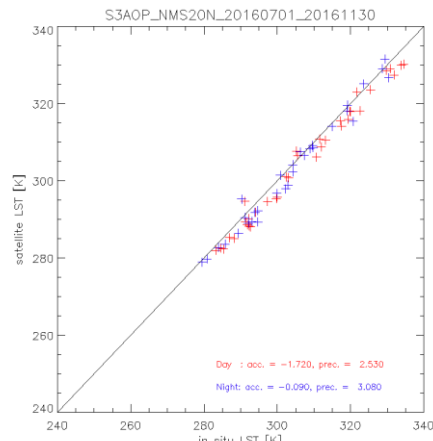
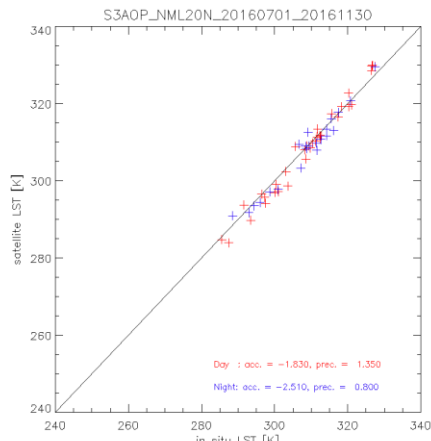
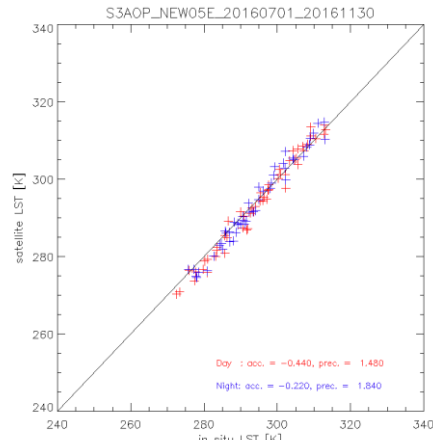
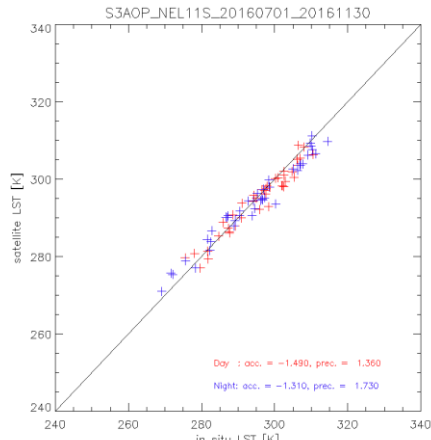


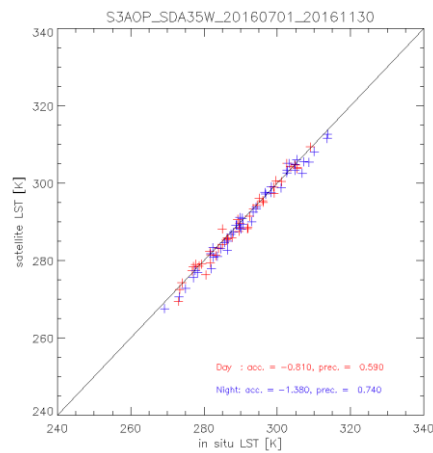
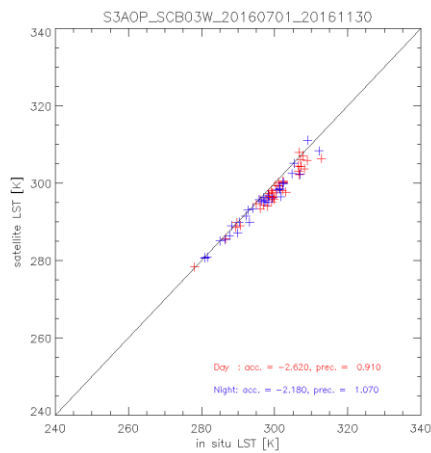
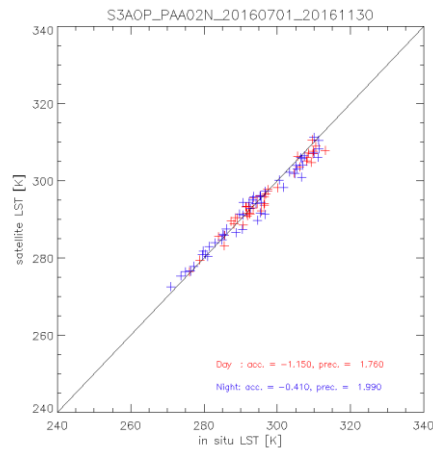
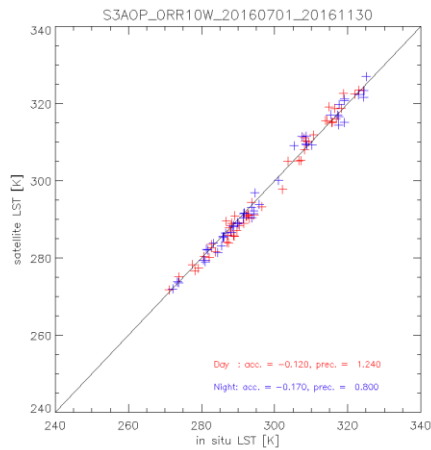
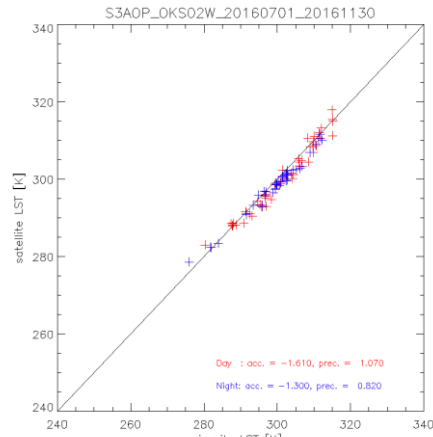
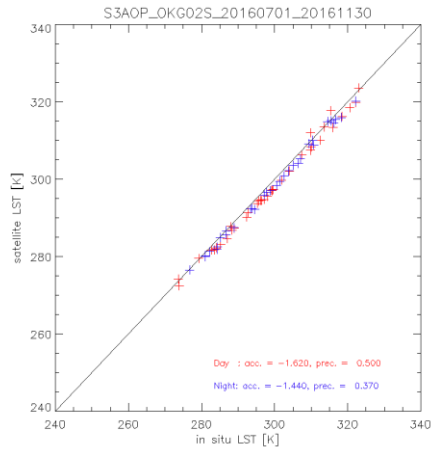


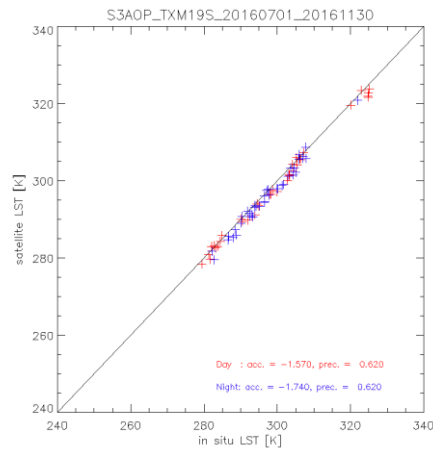
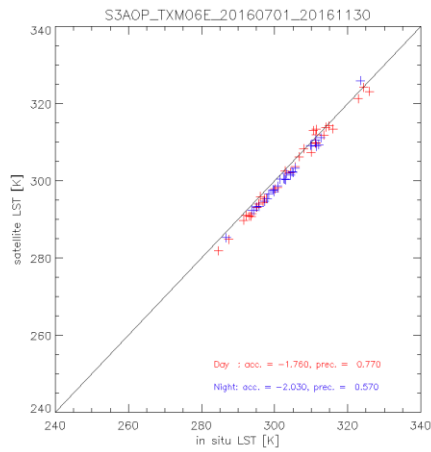
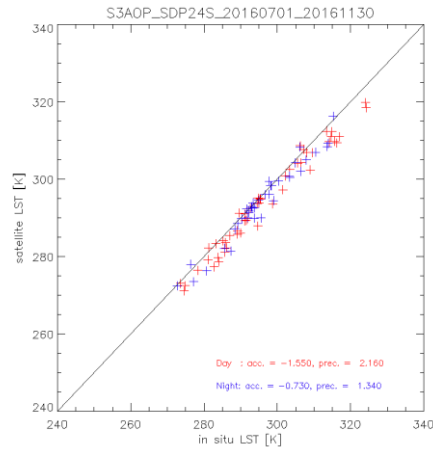
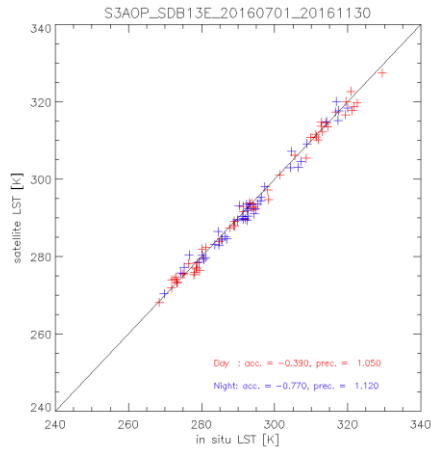












End of document